Causal Deciphering and Inpainting in Spatio-Temporal Dynamics via Diffusion Model

Yifan Duan¹*, Jian Zhao²*, pengcheng⁵, Junyuan Mao¹*, Hao Wu¹, Jingyu Xu³, Shilong Wang¹, Caoyuan Ma³, Kai Wang⁴, Kun Wang⁶†, Xuelong Li²†

¹University of Science and Technology of China, ²TeleAI, China Telecom, ³Wuhan University, ⁴National University of Singapore, ⁵Beijing Forestry University, ⁶Nanyang Technological University {duanyifan28, wslong1259, maojunyuan, wuhao2022}@mail.ustc.edu.cn, {kevinxu, macaoyuan}@whu.edu.cn, pengcheng2022@bjfu.edu.cn, li@nwpu.edu.cn,

wk520529wjh@gmail.com,{E0823044,zhaojian90}@u.nus.edu

Abstract

Spatio-temporal (ST) prediction has garnered a De facto attention in earth sciences, such as meteorological prediction, human mobility perception. However, the scarcity of data coupled with the high expenses involved in sensor deployment results in notable data imbalances. Furthermore, models that are excessively customized and devoid of causal connections further undermine the generalizability and interpretability. To this end, we establish a framework for ST predictions from a causal perspective, termed CaPaint, which targets to identify causal regions in data and endow model with causal reasoning ability in a two-stage process. Going beyond this process, we build on the front door adjustment as the theoretical foundation to specifically address the sub-regions identified as non-causal in the upstream phase. By using a fine-tuned unconditional Diffusion Probabilistic Model (DDPM) as the generative prior, we <u>in-fill</u> the masks defined as environmental parts, offering the possibility of reliable extrapolation for potential data distributions. CaPaint overcomes the high complexity dilemma of optimal ST causal discovery models by reducing the data generation complexity from exponential to quasi-linear levels. Extensive experiments conducted on five real-world ST benchmarks demonstrate that integrating the CaPaint concept allows models to achieve improvements ranging from 3.7%~77.3%. Moreover, compared to traditional mainstream ST augmenters, CaPaint underscores the potential of diffusion models in ST data augmentation, offering a novel paradigm for this field. Our project is available at CaPaint.

1 Introduction

Deep learning methodologies have achieved groundbreaking success across a wide array of spatiotemporal (ST) dynamics systems [28, 84, 44], which include meteorological forecasting [3, 50, 59, 92], wildfire spread modeling [71, 20], intelligent transportation [29, 27, 87], and human mobility systems [27, 90], to name just a few. Traditional ST dynamics approaches, based on first-principles [4, 53], often come with high computational costs. In contrast, ST dynamic analysis methods based on deep learning are not directly reliant on the explicit expression of physical laws but are data-driven [28, 84, 3, 27], relying on training models with large-scale observable datasets [86, 65, 92].

In a parallel vein, numerous efforts aim to incorporate physical laws into deep networks [35, 8, 54, 31, 81], termed Physics-Informed Neural Networks (PINNs), which blend deep learning principles with physics to address challenges in scientific computing, particularly in fluid dynamics.

38th Conference on Neural Information Processing Systems (NeurIPS 2024).

^{*}Equal contribution

[†]Corresponding authors

PINNs augment traditional neural network models by including a term in the loss function that accounts for the physical laws governing fluid dynamics, such as the Navier-Stokes equations [11]. This ensures that the network's predictions are not only consistent with empirical data but also comply with the fundamental principles of fluid dynamics. However, the off-the-shelf PINNs often suffer from limited generalization capabilities, primarily due to their *customized loss function* designs and the *neglect of specific network parameter* contexts [70, 16].

To date, the data-driven deep models are still dominant in ST dynamical systems, where the numerical simulation methods and PINNs generally lag behind. The reason may stem from the rise of large models [1, 76, 28] and the high costs associated with collecting ST data from sensors [93, 39], which creates a significant conflict between the increasing size of *data-hungry* models and the *uneven*, *insufficient* data collection. To this end, in the ST domain, there is looming research aimed at enhancing the causality and interpretability of models.

Unfortunately, research into causality within the field of ST dynamics is lagging. Although some work has considered causal design, due to specific domain constraints and architectural design, it can only enhance the tailor-made capabilities of the model for specific tasks [95, 38]. Moreover, causal discovery tools [12, 15] applied to ST systems often confront the "curse of dimensionality" issue during dimension reduction, despite their effectiveness in elucidating causal relationships from statistical data [75, 47]. Furthermore, NuwaDynamics [82] for the first time proposed decomposing causal and non-causal regions in ST sequences and enhancing the robustness and generalizability of downstream model training by generating more potential distribution ST sequences through mixup [100]. CauSTG [106] and CaST [95] address the issue of ST distribution shifts by implicitly modeling the time series embeddings and employing intervention techniques to observe these shifts.

Though promising, CauSTG [106] and CaST [95] focus on modeling graph-related data, they lack an understanding of high-dimensional observational data (Dimension D < 256). NuwaDynamics, on the other hand, explores all environments through backdoor adjustments [51], generating a vast number of sequences, which lead to nearly $\mathcal{O}(T \times \mathcal{N}_E^{\mathcal{M}(*)})$ training complexity (T represents history time step, \mathcal{N}_E and $\mathcal{M}(*)$ are the number of the environmental patches and mixup, respectively).

In light of this, we propose a general causal structure plugin, termed *CaPaint*, designed to decipher causal regions in ST data without adding extra computational cost, while intervening in non-causal areas to boost the model's generalizability and interpretability. Specifically, our method employs a straightforward approach to causal deciphering, utilizing a vision transformer architecture [33] for self-supervised ST data reconstruc-

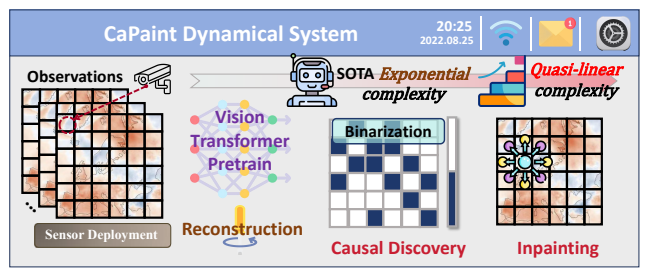


Figure 1: Illustration of the CaPaint overview and advantage across SOTA ST causal model on complexity.

tion. During reconstruction, we leverage *attention scores* from the self-attention mechanism [23] to map onto important causal patches, thus endowing the model with interpretability. By ranking the entire set of importance scores, we define those with lower scores as environmental patches, which contribute minimally to the model. Building on this, we perform **causal interventions** in these environmental areas to aid the model in understanding more latent, complex, and imperceptible distributions, thereby enhancing the overall generalizability of the model (see Figure 1). Concretely, we mask trivial regions and perform generation using DDPM [24, 32] fine-tuned on specific ST data, which can also be interpreted as a ST data inpainting approach.

Insight. • CaPaint obeys the causal deciphering, and guided by the principle of frontdoor adjustment [51, 52] from causal theory, CaPaint performs diffusion inpainting interventions on the environmental (non-causal) diffusion patches while reducing the temporal complexity to a manageable $\mathcal{O}(T \times \mathcal{N}_{\mathcal{E}})$ (from $\mathcal{O}(T \times \mathcal{N}_{E}^{\mathcal{M}(*)})$) in [82]). • CaPaint performs regional inpainting in a more natural manner, avoiding the predicament of repeatedly selecting and perturbing environmental patches. Through diffusion inpainting [42], it generates images that are more aligned with the global distribution. • CaPaint can be understood as a ST augmenter, offering a more rational concept of ST enhancement without disrupting the inherent distribution characteristics of space and time [85]. Our major contributions can be summarized as follow:

- In this paper, we introduce a novel causal structure plugin, CaPaint, which leverages the concept of frontdoor adjustment from causal theory. CaPaint enables various backbone models to learn from a broader distribution of data while providing enhanced interpretability for the models' predictions.
- By integrating diffusion generative models with ST dynamics, CaPaint selectively perturbs noncausal regions while maintaining the integrity of core causal areas. This approach generates valuable and reliable data for scenarios where high-quality data are scarce.
- We conduct extensive experiments across five diverse and representative datasets from different domains, utilizing seven backbone models to assess the effectiveness of the CaPaint method. The empirical results demonstrate that CaPaint consistently enhances performance on all tested datasets and across all backbone models (3.7%~77.3%).

2 Related work & Technical Background

Spatio-temporal Predictive Learning: Various architectures have achieved significant predictive performance in ST domain, which can primarily be categorized as follows: CNN-based models utilize convolutional layers to effectively capture spatial features [45, 48, 77, 9]. RNN-based models, are capable of processing temporal sequence data and are well-suited for understanding temporal changes, showing excellent performance in the prediction of action continuity [69, 80, 86, 72]. GNN-based models effectively capture spatial dependencies and temporal dynamics in data, making them suitable for complex tasks involving geographic locations and temporal changes [44, 25, 36, 17, 99, 98, 83, 14]. Transformer-based models employ self-attention mechanisms to process sequential data in parallel, enhancing the learning of long-term dependencies, and have been used for ST data prediction in complex scenarios [2, 19, 89, 91, 10, 88].

Causal inference: causal discovery algorithms, originally devised for unstructured random vectors [66, 104], have progressively been adapted for ST data analysis [75, 47]. Within the extensive field of deep learning research, the study of causal inference aims to ensure a more stable and robust learning and reasoning paradigm. Recently, an array of techniques has been developed to delve into the nuances of causal features [60, 61, 43, 97], identifying and eliminating spurious correlations [21, 34, 56].

Generative models especially diffusion-based model has gained significant popularity particularly in image and video generation [24, 64, 62]. Sampling optimization algorithms have been used to accelerate the sampling process of diffusion models, significantly reducing the number of steps while improving efficiency. [67, 41]. Additionally, generative models have also been applied to 3D scene generation and point cloud processing, as demonstrated in [40, 30, 73, 74, 22, 63]

Image Inpainting is a technique used to fill in missing or damaged parts of an image. This field can be broadly categorized into the following types. VAE-based methods: These methods leverage Variational Autoencoders to balance diversity and reconstruction [101, 103, 26]. GAN-based methods: Since the introduction of Generative Adversarial Networks, these methods have been widely used for image inpainting [55, 102, 49]. Diffusion model-based methods: Diffusion models have recently shown outstanding performance in image inpainting [46, 68, 57].

3 Methodology

In this section, we systematically introduce causal structure plugin, CaPaint. Initially, we elucidate the methods employed in the upstream phase to delineate causal and non-causal regions (Sec 3.1). Subsequently, we showcase the theoretical underpinnings supporting the CaPaint (Sec 3.2). Building on this causal theory, we further engage in causal intervention within observational data (Sec 3.3). Lastly, we demonstrate how sampling-enhanced ST observations can benefit the complexity of the model's on-device deployment (Sec 3.4).

Problem Formulation. In ST settings, We represent ST observations as a sequence $\{X_t\}_{t=1}^T$, where each observation $X_t \in \mathbb{R}^{H \times W \times C_{\text{in}}}$ originates from these sequences. Our objective is to predict the trajectory for the forthcoming K steps, denoted as $\{X_{t+1}\}_{t=T}^{T+K}$, with each future state X_{t+k} mapped within $\mathbb{R}^{H \times W \times C_{\text{out}}}$. Here, H and W indicate the spatial grid dimensions, while C_{in} and C_{out} define the input and output dimensionality of the observations, respectively.

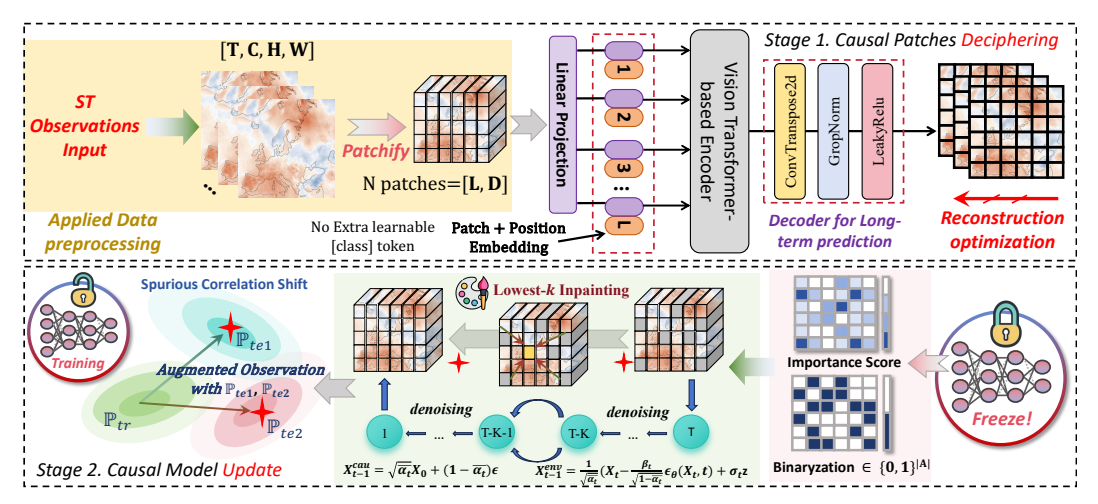


Figure 2: The details of CaPaint. (*Upper.*) The initial phase of discovering causal patches. (*Bottom.*) The update phase designed to eliminate spurious correlation shifts. Following the upstream training of the ViT, a diffusion model is trained in parallel. Using the identified causal patches as conditions, this generative model then performs inpainting for generating multiple sequences.

3.1 Causal Deciphering

To find the causal (non-causal) patches with **no labels**, we employ a self-supervised reconstruction approach based on the Vision Transformer (ViT) [13] to identify key regions within ST observations. ViT segments the image into multiple patches and calculates the relationships between them using a self-attention mechanism. Due to no label property, we intentionally omit the use of the [Cls] token in classification task and send data into ViT for encouraging "local-to-global" reconstruction.

Specifically, each ST data X_t , is divided into $N = HW/p^2$ patches, where each patch $x_t^{patch} \in \mathbb{R}^{N \times (p^2 \times C_{\rm in})}$, with (H,W) being the resolution of the original ST data and (p,p) the resolution of each patch. Subsequently, each patch is mapped to a D-dimensional token through a learnable linear layer, incorporating position embedding to enhance the model's sensitivity to positional information. These tokens are then fed into successive L stacked transformer blocks, as described in Equation 1:

$$L \times \left(X' = \underbrace{X + \text{MSA}(\text{LN}(X))}_{\text{Multi-head Attention}} \Rightarrow X_{\text{out}} = X' + \underbrace{\text{MLP}(\text{LN}(X'))}_{\text{Residual Connection}} \right)$$
(1)

where LN denotes layer normalization, and MLP represents multi-layer perceptron. The upstream self-supervised reconstruction task enables the model to learn intrinsic property of ST data. Navigating the MSA mechanism [78, 96], each patch x_t^{patch} derived from the ST observation X_t is transformed into queries q, keys k, and values v, and then calculates the relevance of each patch to others, forming a weighted representation that focuses on the most informative parts. The attention weights $A_{i,j}^h$ stored in the attention map A^h in each head are computed using the scaled dot-product:

$$set {Q, K, V} = X_t \psi_{tr}, \quad A^h = \operatorname{Softmax} \left(\frac{QK^T}{\sqrt{D_h}} \right) = \begin{pmatrix} A_{1,1}^h & \cdots & A_{1,N}^h \\ \vdots & \ddots & \vdots \\ A_{N,1}^h & \cdots & A_{N,N}^h \end{pmatrix}_{A_{l,l}^h \in \{1, 1, N\}}$$
(2)

where $\psi_{tr} \in \mathbb{R}^{N \times 3D_h}$ are the parameter matrices, D_h represents the dimension of each head, Q, K, and V collectively denote the sets of queries q, keys k, and values v. In our approach, the determination of causal patches, is driven by an analysis of the attention maps A. Each row in an attention map is normalized and represents the importance of other patches relative to the current patch x_t^i . However, to ascertain the overall importance of each patch across the entire input, we aggregate the contributions by summing the values along the columns of the A. To integrate insights across multiple heads, we sum these measures across all heads and then normalize the resultant vector to derive a comprehensive importance score for each patch:

$$S \in \mathbb{R}^N = \text{Softmax}\left(\sum_{h=1}^H \sum_{i=1}^N A_{i,j}^h\right)$$
 (3)

where S represents the normalized importance score vector, $A_{i,j}^h \in A$ denotes the attention that x_t^i pays to x_t^j for each head, H is the number of heads. We sort the importance scores in S and select the patches corresponding to the lowest K scores as environmental patches storing in O_e . The remaining patches are considered causal patches O_c :

$$O_{c} = \operatorname{Topk}\left(\lceil \mathcal{C}(S) \times \epsilon \% \rceil, \ \operatorname{arg\,max}_{S_{i} \in S} \left\{ \operatorname{set}\left(\Psi\left(X_{t}\right)\right)\right) \right\}\right) \tag{4}$$

where C(S) is the counting function, ϵ represents the proportion of patches selected as causal, and $\Psi(X_t)$ denotes the set of patches in the ST observation X_t . We identify the causal patches by locating the indices with the highest values in S and define the non-causal parts as the environmental parts. Our goal is to perform causal interventions on the environmental parts.

3.2 Backdoor Adjustment v.s Frontdoor Adjustment

To address issues of ST data scarcity and poor transferability, we examine the evaluation process using a Structural Causal Model (SCM) [52], as shown in Fig 3. We represent abstract data variables by nodes, with directed links symbolizing causality. The SCM illustrates the interaction among variables through a graphical definition of causation, demonstrating the interconnected nature of these elements. As depicted in the left part, NuwaDynamics employs the backdoor adjustment to enhance the model's generalization performance:

- $\mathcal{X}_{\mathcal{C}} \leftarrow \mathcal{X} \rightarrow \mathcal{X}_{\setminus \mathcal{C}}$. The input \mathcal{X} consists of two disjoint parts $\mathcal{X}_{\mathcal{C}}$ (causal part) and $\mathcal{X}_{\setminus \mathcal{C}}$ (environmental or trivial part).
- $\mathcal{X}_{\mathcal{C}} \to \mathcal{Y} \not\leftarrow \mathcal{X}_{\setminus \mathcal{C}}$. Here, $\mathcal{X}_{\mathcal{C}}$ represents the sole endogenous parent that determines the ground truth \mathcal{Y} . However, in practical scenarios, $\mathcal{X}_{\setminus \mathcal{C}}$ is also employed in predicting \mathcal{Y} , which leads to the formation of spurious associations.

In general, a model \mathcal{F}_{\emptyset} trained using Empirical Risk Minimization (ERM) often struggles to generalize to the test data $\mathcal{D}_{te} \sim \mathbb{P}_{te}$. Such distribution shifts are often induced by variations in environmental patches. Hence, addressing the confounding effect caused by the environmental confounder is crucial. Backdoor adjustment techniques are employed to perturb the environmental components, thereby enhancing the model's potential to observe a broader range of latent distributions by forcibly perturbing the environmental variables $\mathcal{X}_{\setminus\mathcal{C}}$ (referred to as the **do-calculus** [51] operator). Unfortunately,

• traversing all environmental variables is quite

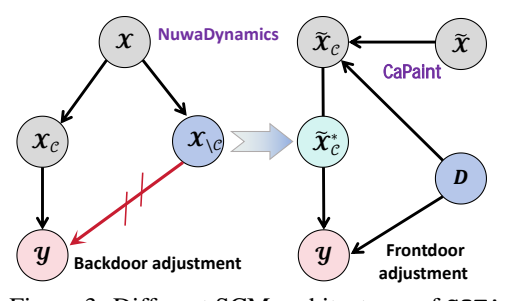


Figure 3: Different SCM architectures of SOTA and CaPaint.

challenging. Although NuwaDynamics uses Gaussian sampling to mitigate the issue of complexity, controlling Gaussian sampling in temporal sequence operations is particularly difficult. It requires meticulous adjustment of mean and variance to ensure a balance between the number of environmental samples and the training burden. ② Worse still, by traversing all environments, it likely violates underlying properties, including distribution shift content and nonexistent scenarios [94]. To address this issue, we employ front-door adjustment, as illustrated in the right half of the Fig 3:

- $\tilde{\mathcal{X}}_{\mathcal{C}} \leftarrow \mathcal{D} \rightarrow \mathcal{Y}$. In this structure, \mathcal{D} serves as a confounder, creating a misleading path between $\tilde{\mathcal{X}}_{\mathcal{C}}$ and \mathcal{Y} . Here, $\tilde{\mathcal{X}}_{\mathcal{C}}$ represents the causal component within $\tilde{\mathcal{X}}$.
- $\tilde{\mathcal{X}}_{\mathcal{C}} \to \tilde{\mathcal{X}}_{\mathcal{C}}^* \to \mathcal{Y}$. $\tilde{\mathcal{X}}_{\mathcal{C}}^*$ acts as the surrogate variable of $\tilde{\mathcal{X}}_{\mathcal{C}}$ and completes $\tilde{\mathcal{X}}_{\mathcal{C}}$ to align it with the data distribution. Initially, it derives from and encompasses $\tilde{\mathcal{X}}_{\mathcal{C}}$. Specifically, it envisions the potential complete observations that should exist when observing the sub-counterpart $\tilde{\mathcal{X}}_{\mathcal{C}}$. Additionally, $\tilde{\mathcal{X}}_{\mathcal{C}}^*$ adheres to the data distribution and upholds the intrinsic knowledge of graph properties, thus eliminating any link between \mathcal{D} and $\tilde{\mathcal{X}}_{\mathcal{C}}^*$. Consequently, $\tilde{\mathcal{X}}_{\mathcal{C}}^*$ is well-suited to act as the mediator, which in turn influences the model's predictions $(\to \mathcal{Y})$.

In our front-door adjustment framework, we utilize **do-calculus** on the variable $\tilde{\mathcal{X}}_{\mathcal{C}}$ to eliminate the spurious correlations introduced by $\mathcal{D} \to \mathcal{Y}$. Specifically, we achieve this by summing over potential surrogate observations $\tilde{X}_{\mathcal{C}}^*$. This approach allows us to connect two identifiable partial effects: $\tilde{\mathcal{X}}_{\mathcal{C}} \to \tilde{\mathcal{X}}_{\mathcal{C}}^*$ and $\tilde{\mathcal{X}}_{\mathcal{C}}^* \to \mathcal{Y}$:

$$P\left(\mathcal{Y}|do\left(\tilde{\mathcal{X}}_{\mathcal{C}} = \tilde{\mathcal{X}}_{\mathcal{C}}\right)\right) = \sum_{\tilde{\mathcal{X}}_{\mathcal{C}}^{*}} P\left(\mathcal{Y}|do\left(\tilde{\mathcal{X}}_{\mathcal{C}}^{*} = \tilde{\mathcal{X}}_{\mathcal{C}}^{*}\right)\right) P\left(\tilde{\mathcal{X}}_{\mathcal{C}}^{*} = \tilde{\mathcal{X}}_{\mathcal{C}}^{*}|do\left(\tilde{\mathcal{X}}_{\mathcal{C}} = \tilde{\mathcal{X}}_{\mathcal{C}}\right)\right)$$

$$= \sum_{\tilde{\mathcal{X}}_{\mathcal{C}}^{*}} \sum_{\tilde{\mathcal{X}}_{\mathcal{C}}^{'}} P\left(\mathcal{Y}\Big|\tilde{\mathcal{X}}_{\mathcal{C}}^{*} = \tilde{\mathcal{X}}_{\mathcal{C}}^{*}; \tilde{\mathcal{X}}_{\mathcal{C}} = \tilde{\mathcal{X}}_{\mathcal{C}}^{'}\right) P\left(\tilde{\mathcal{X}}_{\mathcal{C}} = \tilde{\mathcal{X}}_{\mathcal{C}}^{'}\right) P\left(\tilde{\mathcal{X}}_{\mathcal{C}}^{*} = \tilde{\mathcal{X}}_{\mathcal{C}}^{*}\Big|do\left(\tilde{\mathcal{X}}_{\mathcal{C}} = \tilde{\mathcal{X}}_{\mathcal{C}}\right)\right)$$

$$= \sum_{\tilde{\mathcal{X}}_{\mathcal{C}}^{*}} \sum_{\tilde{\mathcal{X}}_{\mathcal{C}}^{'}} P\left(\mathcal{Y}\Big|\tilde{\mathcal{X}}_{\mathcal{C}}^{*} = \tilde{\mathcal{X}}_{\mathcal{C}}^{*}; \tilde{\mathcal{X}}_{\mathcal{C}} = \tilde{\mathcal{X}}_{\mathcal{C}}^{'}\right) P\left(\tilde{\mathcal{X}}_{\mathcal{C}} = \tilde{\mathcal{X}}_{\mathcal{C}}^{'}\right) P\left(\tilde{\mathcal{X}}_{\mathcal{C}}^{*} = \tilde{\mathcal{X}}_{\mathcal{C}}^{*}\Big|\tilde{\mathcal{X}}_{\mathcal{C}} = \tilde{\mathcal{X}}_{\mathcal{C}}\right)$$

$$(5)$$

 $P\left(\tilde{\mathcal{X}}^*_{\mathcal{C}}|do\left(\tilde{\mathcal{X}}_{\mathcal{C}}=\tilde{X}_{\mathcal{C}}\right)\right)=P\left(\tilde{\mathcal{X}}^*_{\mathcal{C}}|\tilde{\mathcal{X}}_{\mathcal{C}}=\tilde{X}_{\mathcal{C}}\right) \text{ holds as } \tilde{\mathcal{X}}_{\mathcal{C}} \text{ is the only parent of } \tilde{\mathcal{X}}^*_{\mathcal{C}}. \text{ With data pair } (\tilde{\mathcal{X}}_{\mathcal{C}},\tilde{\mathcal{X}}^*_{\mathcal{C}}), \text{ we can feeding the surrogate observations } \tilde{\mathcal{X}}^*_{\mathcal{C}} \text{ into our ST framework, conditional on the } \tilde{\mathcal{X}}_{\mathcal{C}}, \text{ to estimate } P\left(\mathcal{Y} \middle| \tilde{\mathcal{X}}^*_{\mathcal{C}}=\tilde{\mathcal{X}}^*_{\mathcal{C}}; \tilde{\mathcal{X}}_{\mathcal{C}}=\tilde{\mathcal{X}}^*_{\mathcal{C}}\right). \text{ Compared to previous work NuwaDynamics, CaPaint}$

utilizes causal regions to generate global surrogate variables in a more rational manner, circumventing the cumbersome need to traverse environmental variables inherent in backdoor adjustments. **In fact, backdoor adjustments often likely violate underlying properties, leading to the generation of non-existent data distributions.** The broader scenarios of CaPaint will be detailed in Appendix C.

3.3 Causal Intervention via Diffusion Inpainting

Building on the principles of causal analysis outlined above, we proceed to perform interventions on the environmental patches using diffusion inpainting, which enables us to manipulate the environmental areas. Initially, given the unique complexities of ST datasets, we *fine-tune* the diffusion parameters to adapt seamlessly to the domain-specific challenges, which enhances the accuracy of our interventions on environmental patches. Diffusion models learn the distribution of data through a forward noise addition process and a reverse denoising process:

$$q(X_t \mid X_{t-1}) = \mathcal{N}(X_t; \sqrt{1 - \beta_t} X_{t-1}, \beta_t I), \quad p_{\theta}(X_{t-1} \mid X_t) = \mathcal{N}(X_{t-1}; \mu_{\theta}(X_t, t), \Sigma_{\theta}(X_t, t))$$
 (6)

where X_t represents the data state at time step t, undergoing a transformation from its previous state x_{t-1} , β_t controls the variance of the noise added at each step in the forward process, μ_{θ} and Σ_{θ} are neural network outputs that approximate the mean and covariance, respectively. The fine-tuning objective of the diffusion process is designed to approximate the data distribution more accurately. Specifically, the training objective for diffusion models, denoted as ϵ_{θ} , which predicts the noise, is typically defined as a simplified version of the variational bound:

$$L_{\text{simple}} = \mathbb{E}_{X_0, \epsilon \sim \mathcal{N}(\mathbf{0}, \mathbf{I}), \mathbf{c}, t} \| \epsilon - \epsilon_{\theta} (X_t, \mathbf{c}, t) \|^2$$
(7)

where c is the condition information. In this paper, we perform inpainting on the environmental patches of ST data. Inspired by [42], we generate a mask image for each ST data where the causal patches are black and the environmental patches are white. By independently sampling the causal and environmental patches and applying the diffusion inpainting process, we are able to generate augmented ST observation data. The detailed algorithmic process is shown in Appendix A.

$$X_{t-1}^{cau} = \sqrt{\bar{\alpha}_t} X_0 + (1 - \bar{\alpha}_t) \epsilon, \quad X_{t-1}^{env} = \frac{1}{\sqrt{\alpha_t}} \left(X_t - \frac{\beta_t}{\sqrt{1 - \bar{\alpha}_t}} \epsilon_{\theta}(X_t, t) + \sigma_t z \right)$$
(8)

$$X_{t-1} = m \odot X_{t-1}^{cau} + (1-m) \odot X_{t-1}^{env}$$
(9)

where X^{cau} and X^{env} denote causal patches and environmental patches, m is a binary mask matrix, α_t represents the scaling factor at each diffusion step, determining the variance retained in the transition from X_{t-1} to X_t . The cumulative product $\bar{\alpha}_t = \prod_{i=1}^t \alpha_i$ represents the accumulated scaling effect from the T=0 to step t. Equation 9 illustrates the merging of environmental patches and causal patches. Finally, the enhanced ST observation data are stored within our temporal sequence repository to bolster the downstream backbone.

3.4 ST Sequence Sampling Modeling

Previous work [82] assumed that the closer the time point is to the present, the greater its influence, and thus used Gaussian sampling to select more ST data closer to the current time point. However, we argue that uniform sampling can better enhance the model's generalization ability. To enhance computational efficiency while ensuring prediction accuracy, we employ a ST sequence modeling approach that samples at each time point with a fixed probability controlled by the hyperparameter p. This method allows us to sample from both original and generated data at each time point, thereby creating a new spatiotemporal sequence. We use two hyperparameters: p, which controls the sampling probability, and r, which determines the number of generated spatiotemporal sequences, achieving an optimal balance between computational efficiency and prediction accuracy. The specific sampling process can be represented by the following equation:

$$X_t' = \operatorname{Sample}(X_t, p, r) \tag{10}$$

where X_t represents the collection of original and generated data at time point t, and Sample(X_t , p) denotes the dataset obtained by sampling from X_t with probability p. The hyperparameter p is directly set as the sampling probability, while r is used to specify the number of generated ST sequences.

4 Experiments

In this section, we will validate the effectiveness of our proposed causal structure plugin, CaPaint. We design four research questions (RQs) to comprehensively evaluate the performance of CaPaint: **RQ1:** Does CaPaint effectively enhance model performance and applicability? **RQ2:** How does CaPaint perform in data-scarce scenarios? **RQ3:** How does the performance of CaPaint compare with other augmentation methods? **RQ4:** Is CaPaint effective for long-term time step predictions? Through these research questions, we aim to validate the effectiveness and advantages of CaPaint in handling ST data from multiple perspectives.

4.1 Experimental settings

Datasets. We extensively evaluate our proposal using a diverse range of benchmark datasets spanning multiple fields, include FireSys [7], SEVIR [79], Diffusion reaction system (DRS) [6], KTH [58] and TaxiBJ+ [37]. Specifically, FireSys represents fire dynamics, SEVIR covers meteorological events, DRS involves physical control systems, KTH focuses on human motion dynamics, and TaxiBJ+ is a transportation dataset. Detailed information can be found in the Appendix B.

Backbones and Metrics To validate the generalizability of CaPaint, we select multiple model frameworks for our experiments, including the classic model like ConvLSTM [65], PredRNN-V2 [86], Vision Transformer (ViT) [13], MAU [5], the efficiency-focused SimVP [18], and some of the latest models like MmvP [105] and Earthfarsser [92]. Our evaluation metrics include mean absolute error (MAE), mean squared error (MSE), and structural similarity index measure (SSIM). Detailed information can be found in the Appendix D.

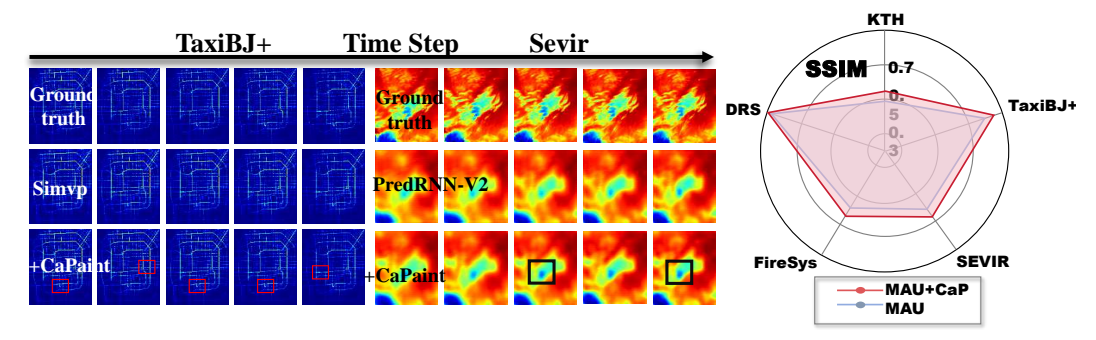


Figure 4: Visualization of prediction results for TaxiBJ+ and SEVIR datasets. The left side shows the predicted results of the last 5 frames for TaxiBJ+. The middle presents the results of long-term predictions for SEVIR, displaying the last five frames from step $10 \rightarrow$ step 20. The right side compares SSIM metrics with and without the incorporation of CaPaint.

107610

Table 1: This table showcases the results (five runs) differences between using the CaPaint concept (+CaP) and not using it (Ori) across various datasets. All MAE and MSE values are multiplied by 100. Blue and Red backgrounds indicate the percentage improvement (reduction) in MAE and MSE, respectively.

Backbone $(10 \rightarrow 10)$	Metric	TaxiBJ+		КТН		SEVIR		DRS		FireSys	
		Ori	+CaP	Ori	+CaP	Ori	+CaP	Ori	+CaP	Ori	+CaP
ViT [13]	MAE	16.59	14.54	32.03	29.52	18.69	17.56	13.59	7.52	17.32	15.97
	MSE	11.40	8.89	36.11	32.79	9.93	9.16	6.21	1.41	23.40	21.06
		12.4% 1	22.1% ↑	7.8% ↑	9.2% ↑	6.1% ↑	7.7% ↑	44.7% ↑	77.3% ↑	7.8% ↑	$10.1\% \uparrow$
Earthfarsser [92]	MAE	14.57	12.75	23.56	20.59	15.23	14.47	2.03	1.44	17.15	16.29
	MSE	9.94	7.83	16.84	14.07	6.75	6.01	4.09	2.24	23.37	21.94
		12.5% 1	21.2% ↑	$12.6\% \uparrow$	16.4% ↑	5.0% ↑	10.9% ↑	29.1% ↑	37.8% ↑	$5.1\% \uparrow$	6.1% ↑
Mmvp [105]	MAE		16.17	30.62	27.57	20.67	17.21	15.05	11.02	19.37	18.16
	MSE	14.22	12.29	27.31	22.37	8.45	7.26	4.11	2.32	26.09	24.97
	Δ				18.1% ↑	16.7% ↑	14.1% ↑	$26.8\% \uparrow$	43.6% ↑	6.2% ↑	4.3% ↑
	MAE	18.22		22.77	20.03	20.51	18.41	5.43	3.89	22.22	10.08
ConvLSTM [65]	MSE	16.79	14.67	27.37	25.15	12.12	11.41	0.64	0.31	28.64	26.44
			$12.6\% \uparrow$	12.1% ↑	8.1% ↑	10.2% ↑	5.9% ↑	28.3% ↑	51.6% ↑	9.6% ↑	7.6% ↑
PredRNN-V2 [86]	MAE	14.18	13.05	26.73	23.64	17.94	16.26	8.76	7.98	18.26	16.14
		9.60	7.89	21.45	19.11	8.54	7.73	4.37	4.18	24.71	23.12
	Δ		$16.6\% \uparrow$	11.6% ↑	10.9% ↑	9.3% ↑	9.4% ↑	8.9% ↑	$4.3\% \uparrow$	11.6% ↑	$6.5\% \uparrow$
MAU [5]	MAE	23.28	20.96	29.54	27.82	25.07	24.14	11.84	9.97	20.67	18.65
	MSE	20.46	16.60	30.19	27.84	15.43	14.34	5.28	4.66	30.89	28.91
			18.9% ↑	5.9% ↑	7.8% ↑	3.7% ↑	7.1% ↑	15.8% ↑	11.8% ↑	9.8% ↑	$6.4\% \uparrow$
SimVP [18]	MAE	15.91	13.45	23.21	20.56	15.48	14.63	2.12	1.57	17.01	15.79
	MSE	10.96	8.21	16.46	13.91	6.82	6.21	9.54	5.03	23.34	22.11
	Δ	15.4% 1	$25.1\% \uparrow$	11.4% ↑	$15.3\% \uparrow$	5.5% ↑	8.9% ↑	$25.9\% \uparrow$	47.3% ↑	8.4% ↑	5.3% ↑

4.2 Evaluating the Efficacy of CaPaint (RQ1 & RQ4)

In this section, we conduct extensive experiments to demonstrate the effectiveness of the *CaPaint* method. For Transformer architectures, we can directly transfer the model parameters trained in upstream tasks, thereby achieving efficient downstream training. For non-Transformer architectures, we focus on transferring the data itself to train the downstream models. The data presented in the Tab 1 show the performance improvements achieved by generating **only one** single generalized copy for each ST sequence. As shown in the Table 1, we can list the **Obs**ervations:

Obs 1. +CaPaint consistently leads w/o Capaint settings across all datasets. As shown in Table 1 and the right side of Fig 4, we can easily observe that introducing +CaPaint significantly improves model performance on MAE, MSE and SSIM metrics across all datasets. For example, with the ViT model on TaxiBJ+, MAE drops from $16.59 \rightarrow 14.54$, MSE from $11.40 \rightarrow 8.89$; On Diffusion Reaction Systems, MAE significantly decreases from $13.59 \rightarrow 7.52$, MSE from $6.21 \rightarrow 1.41$. This shows CaPaint's effectiveness in boosting performance in various domains.

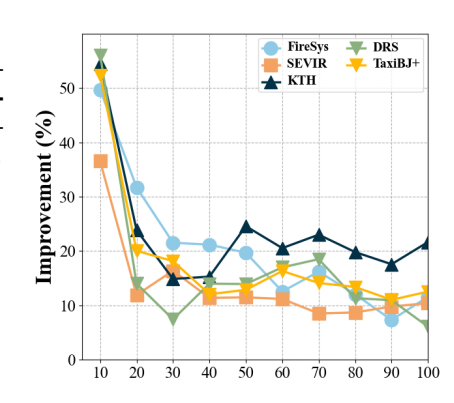
Obs 2. +CaPaint enhances model local insights ST scenarios. By analyzing the left side of Figure 4, we clearly see that the +CaPaint effectively reduces the model's prediction loss. Moreover, it is observed that +CaPaint provides more accurate predictions in finer details, closely aligning with the actual result curves. This demonstrates CaPaint's capability to enhance prediction accuracy and reliability, ensuring that the forecasts closely mirror real-world outcomes.

Obs 3. +CaPaint remains effective in long-Term ST predictions. By analyzing the middle of Figure 4, we observe that +CaPaint continues to demonstrate its effectiveness in long-term time step predictions for ST tasks. For instance, the details in the SEVIR dataset predictions improve significantly, indicating that CaPaint is still applicable and beneficial in challenging ST tasks.

4.3 Performance in Data-Scarce Scenarios (RQ2)

To assess the performance of *CaPaint* in data-scarce scenarios, we conducted experiments using **varying proportions of training data** across multiple datasets and backbones. Specifically, we measured the SSIM improvement at different training data proportions, demonstrating the generalizability and robustness of *CaPaint*.

Obs 1. CaPaint shows consistent improvements across all training data proportions. As shown in Figures 5 and 6, *CaPaint* consistently improves SSIM across all



training data proportions. This indicates that CaPaint is effective regardless of the amount of training data available, reinforcing its versatility and applicability in diverse scenarios.

Obs 2. Significant performance gains in low data scenarios. The results indicate that CaPaint yields substantial performance improvements, especially in low data scenarios. For instance, with only 10% of the training data, the SSIM improvement is most pronounced, highlighting the method's effectiveness in data-scarce environments. For example, in the TaxiBJ+ dataset with ViT backbone, the SSIM improvement reaches up to more than 50%, showcasing CaPaint's capability to enhance model performance with limited data.

Obs 3. Diminishing returns with increased training data. While *CaPaint* consistently enhances performance, the degree of improvement diminishes as the proportion of training data increases. This trend suggests that the primary benefits of *CaPaint* are most evident when data is scarce, but the method remains beneficial even as more data becomes available.

Obs 4. CaPaint demonstrates superior performance with equivalent data volumes. As illustrated in Fig 7, when comparing 25% original plus 25% augmented data with 50% original data, *CaPaint* achieves lower MAE and MSE. This demonstrates that *CaPaint* consistently outperforms the original model by effectively using a mix of original and augmented data, which together match the data volume used by the original model alone.

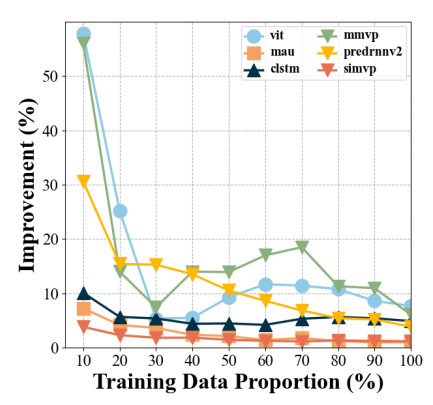


Figure 6: SSIM Improvement on DRS across various backbones

4.4 Performance Comparison (RQ3)

Table 2: Comparison between CaPaint and other data augmentation methods across various datasets.

Datasets	Flip	Rotate	Crop	NuWa	CaPaint
DRS	$2.10_{\pm 0.16}$	$2.11_{\pm 0.19}$	$2.34_{\pm0.26}$	$2.02_{\pm 0.09}$	$1.57_{\pm0.14}$
KTH	$23.15 {\scriptstyle \pm 1.95}$	$23.14 {\scriptstyle \pm 1.67}$	$23.11_{\pm 1.83}$	$22.32_{\pm 0.94}$	$20.56_{\pm 1.02}$
SEVIR	$15.41 {\scriptstyle \pm 1.49}$	$15.45 {\pm} 1.32$	$15.95 {\pm} 1.64$	$15.14 {\scriptstyle \pm 1.57}$	$14.63_{\pm 1.89}$
TaxiBJ+	$16.47 _{\pm 0.99}$	$16.39_{\pm 1.32}$	$15.94_{\pm 1.45}$	$15.11 _{\pm 0.87}$	$12.87_{\pm 0.76}$
FireSys	$17.02_{\pm 2.17}$	$17.07_{\pm 1.94}$	$17.15_{\pm 2.45}$	$16.68_{\pm 1.79}$	$15.79_{\pm 1.88}$

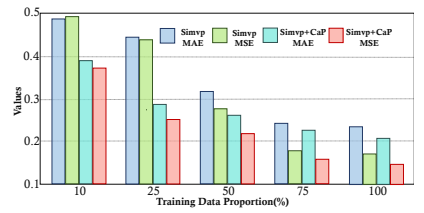


Figure 7: Visualizations in both MAE and MSE with Simvp and + CaP at various training data proportions.

In this section, we compare the performance of different data augmentation methods. Tab 2 shows the model performance using various data augmentation methods across multiple datasets, measured by MAE. It can be seen that traditional data augmentation methods, such as flipping, rotation, and cropping, produce results that are either on par with or slightly worse than the original data. Take the FireSys dataset as an example, MAE increased from $17.01 \rightarrow 17.07$ after rotation augmentation. This indicates that conventional data augmentation methods may **disrupt the intrinsic properties** of ST data, thereby negatively impacting model performance.

In contrast, our method *CaPaint* achieves the best performance **across all datasets**. For instance, on the TaxiBJ+ dataset, the MAE with *CaPaint* augmentation is 12.87, which is significantly better than the MAE of 15.11 with *NuwaDynamics* manual mixup augmentation and the MAE of 15.94 with other traditional augmentation methods such as cropping. These results highlight the advantage of our method in preserving the integrity of ST data properties. CaPaint not only effectively avoids the disruption caused by data augmentation processes on ST data characteristics but also significantly enhances the model's predictive capability.

5 Conclusion & Future Work

In this study, we advance the exploration of applying front-door adjustment and causality principles to spatio-temporal forecasting tasks through the introduction of *CaPaint*. Building upon the foundation of upstream self-supervised learning, we identify causal regions as crucial elements for generating

comprehensive and potential data distributions. By integrating diffusion generative models, we ensure the generated data's rationality and generalizability, thereby enhancing the downstream models' ability to generalize beyond the observed distribution and improving their interpretability. Moving forward, we plan to explore various generative models for the production of arbitrary-channel ST data to enhance the *CaPaint* robustness.

6 Acknowledgement

This work was supported by National Natural Science Foundation of China (62476224).

References

- [1] Josh Achiam, Steven Adler, Sandhini Agarwal, Lama Ahmad, Ilge Akkaya, Florencia Leoni Aleman, Diogo Almeida, Janko Altenschmidt, Sam Altman, Shyamal Anadkat, et al. Gpt-4 technical report. *arXiv preprint arXiv:2303.08774*, 2023.
- [2] Cong Bai, Feng Sun, Jinglin Zhang, Yi Song, and Shengyong Chen. Rainformer: Features extraction balanced network for radar-based precipitation nowcasting. *IEEE Geoscience and Remote Sensing Letters*, 19:1–5, 2022.
- [3] Kaifeng Bi, Lingxi Xie, Hengheng Zhang, Xin Chen, Xiaotao Gu, and Qi Tian. Pangu-weather: A 3d high-resolution model for fast and accurate global weather forecast. *arXiv preprint* arXiv:2211.02556, 2022.
- [4] Marius Bürkle, Umesha Perera, Florian Gimbert, Hisao Nakamura, Masaaki Kawata, and Yoshihiro Asai. Deep-learning approach to first-principles transport simulations. *Physical Review Letters*, 126(17):177701, 2021.
- [5] Zheng Chang, Xinfeng Zhang, Shanshe Wang, Siwei Ma, Yan Ye, Xiang Xinguang, and Wen Gao. Mau: A motion-aware unit for video prediction and beyond. *Advances in Neural Information Processing Systems*, 34:26950–26962, 2021.
- [6] Boyuan Chen, Kuang Huang, Sunand Raghupathi, Ishaan Chandratreya, Qiang Du, and Hod Lipson. Discovering state variables hidden in experimental data. *arXiv preprint arXiv:2112.10755*, 2021.
- [7] Boyuan Chen, Kuang Huang, Sunand Raghupathi, Ishaan Chandratreya, Qiang Du, and Hod Lipson. Automated discovery of fundamental variables hidden in experimental data. *Nature Computational Science*, 2(7):433–442, 2022.
- [8] Yuyao Chen and Luca Dal Negro. Physics-informed neural networks for imaging and parameter retrieval of photonic nanostructures from near-field data. *APL Photonics*, 7(1), 2022.
- [9] Jinguo Cheng, Ke Li, Yuxuan Liang, Lijun Sun, Junchi Yan, and Yuankai Wu. Rethinking urban mobility prediction: A super-multivariate time series forecasting approach. arXiv preprint arXiv:2312.01699, 2023.
- [10] Jinguo Cheng, Chunwei Yang, Wanlin Cai, Yuxuan Liang, and Yuankai Wu. Nuwats: Mending every incomplete time series. *arXiv preprint arXiv:2405.15317*, 2024.
- [11] Peter Constantin and Ciprian Foiaş. *Navier-stokes equations*. University of Chicago press, 1988.
- [12] Giorgia Di Capua, Jakob Runge, Reik V Donner, Bart van den Hurk, Andrew G Turner, Ramesh Vellore, Raghavan Krishnan, and Dim Coumou. Dominant patterns of interaction between the tropics and mid-latitudes in boreal summer: Causal relationships and the role of time-scales. *Weather and Climate Dynamics Discussions*, 2020:1–28, 2020.
- [13] Alexey Dosovitskiy, Lucas Beyer, Alexander Kolesnikov, Dirk Weissenborn, Xiaohua Zhai, Thomas Unterthiner, Mostafa Dehghani, Matthias Minderer, Georg Heigold, Sylvain Gelly, et al. An image is worth 16x16 words: Transformers for image recognition at scale. *arXiv* preprint arXiv:2010.11929, 2020.

- [14] Yifan Duan, Guibin Zhang, Shilong Wang, Xiaojiang Peng, Wang Ziqi, Junyuan Mao, Hao Wu, Xinke Jiang, and Kun Wang. Cat-gnn: Enhancing credit card fraud detection via causal temporal graph neural networks. *arXiv* preprint arXiv:2402.14708, 2024.
- [15] Imme Ebert-Uphoff and Yi Deng. Causal discovery from spatio-temporal data with applications to climate science. In 2014 13th International Conference on Machine Learning and Applications, pages 606–613. IEEE, 2014.
- [16] Stathi Fotiadis, Mario Lino Valencia, Shunlong Hu, Stef Garasto, Chris D Cantwell, and Anil Anthony Bharath. Disentangled generative models for robust prediction of system dynamics. 2023.
- [17] Xiaowei Gao, Xinke Jiang, Dingyi Zhuang, Huanfa Chen, Shenhao Wang, Stephen Law, and James Haworth. Uncertainty-aware probabilistic graph neural networks for road-level traffic accident prediction. 2023. URL https://api.semanticscholar.org/CorpusID: 261681823.
- [18] Zhangyang Gao, Cheng Tan, Lirong Wu, and Stan Z Li. Simvp: Simpler yet better video prediction. In *Proceedings of the IEEE/CVF conference on computer vision and pattern recognition*, pages 3170–3180, 2022.
- [19] Zhihan Gao, Xingjian Shi, Hao Wang, Yi Zhu, Yuyang Bernie Wang, Mu Li, and Dit-Yan Yeung. Earthformer: Exploring space-time transformers for earth system forecasting. *Advances in Neural Information Processing Systems*, 35:25390–25403, 2022.
- [20] Sebastian Gerard, Yu Zhao, and Josephine Sullivan. Wildfirespreadts: A dataset of multi-modal time series for wildfire spread prediction. Advances in Neural Information Processing Systems, 36, 2024.
- [21] Ishaan Gulrajani and David Lopez-Paz. In search of lost domain generalization. *arXiv preprint arXiv:2007.01434*, 2020.
- [22] Ziyu Guo, Renrui Zhang, Xiangyang Zhu, Yiwen Tang, Xianzheng Ma, Jiaming Han, Kexin Chen, Peng Gao, Xianzhi Li, Hongsheng Li, et al. Point-bind & point-llm: Aligning point cloud with multi-modality for 3d understanding, generation, and instruction following. *arXiv* preprint arXiv:2309.00615, 2023.
- [23] Kai Han, Yunhe Wang, Hanting Chen, Xinghao Chen, Jianyuan Guo, Zhenhua Liu, Yehui Tang, An Xiao, Chunjing Xu, Yixing Xu, et al. A survey on vision transformer. *IEEE transactions on pattern analysis and machine intelligence*, 45(1):87–110, 2022.
- [24] Jonathan Ho, Ajay Jain, and Pieter Abbeel. Denoising diffusion probabilistic models. *Advances in neural information processing systems*, 33:6840–6851, 2020.
- [25] Xinke Jiang, Dingyi Zhuang, Xianghui Zhang, Hao Chen, Jiayuan Luo, and Xiaowei Gao. Uncertainty quantification via spatial-temporal tweedie model for zero-inflated and long-tail travel demand prediction. *Proceedings of the 32nd ACM International Conference on Information and Knowledge Management*, 2023. URL https://api.semanticscholar.org/CorpusID:259187717.
- [26] Xinke Jiang, Zidi Qin, Jiarong Xu, and Xiang Ao. Incomplete graph learning via attribute-structure decoupled variational auto-encoder. *Proceedings of the 17th ACM International Conference on Web Search and Data Mining*, 2024. URL https://api.semanticscholar.org/CorpusID:268319406.
- [27] Guangyin Jin, Yuxuan Liang, Yuchen Fang, Zezhi Shao, Jincai Huang, Junbo Zhang, and Yu Zheng. Spatio-temporal graph neural networks for predictive learning in urban computing: A survey. *IEEE Transactions on Knowledge and Data Engineering*, 2023.
- [28] Ming Jin, Qingsong Wen, Yuxuan Liang, Chaoli Zhang, Siqiao Xue, Xue Wang, James Zhang, Yi Wang, Haifeng Chen, Xiaoli Li, et al. Large models for time series and spatio-temporal data: A survey and outlook. *arXiv preprint arXiv:2310.10196*, 2023.

- [29] Sepideh Kaffash, An Truong Nguyen, and Joe Zhu. Big data algorithms and applications in intelligent transportation system: A review and bibliometric analysis. *International journal of production economics*, 231:107868, 2021.
- [30] Animesh Karnewar, Andrea Vedaldi, David Novotny, and Niloy J Mitra. Holodiffusion: Training a 3d diffusion model using 2d images. In *Proceedings of the IEEE/CVF conference on computer vision and pattern recognition*, pages 18423–18433, 2023.
- [31] George Em Karniadakis, Ioannis G Kevrekidis, Lu Lu, Paris Perdikaris, Sifan Wang, and Liu Yang. Physics-informed machine learning. *Nature Reviews Physics*, 3(6):422–440, 2021.
- [32] Tero Karras, Samuli Laine, and Timo Aila. A style-based generator architecture for generative adversarial networks. In *Proceedings of the IEEE/CVF conference on computer vision and pattern recognition*, pages 4401–4410, 2019.
- [33] Salman Khan, Muzammal Naseer, Munawar Hayat, Syed Waqas Zamir, Fahad Shahbaz Khan, and Mubarak Shah. Transformers in vision: A survey. ACM computing surveys (CSUR), 54 (10s):1–41, 2022.
- [34] Pang Wei Koh, Shiori Sagawa, Henrik Marklund, Sang Michael Xie, Marvin Zhang, Akshay Balsubramani, Weihua Hu, Michihiro Yasunaga, Richard Lanas Phillips, Irena Gao, et al. Wilds: A benchmark of in-the-wild distribution shifts. In *International conference on machine learning*, pages 5637–5664. PMLR, 2021.
- [35] Aditi Krishnapriyan, Amir Gholami, Shandian Zhe, Robert Kirby, and Michael W Mahoney. Characterizing possible failure modes in physics-informed neural networks. *Advances in Neural Information Processing Systems*, 34:26548–26560, 2021.
- [36] Rongfang Li, Ting Zhong, Xinke Jiang, Goce Trajcevski, Jin Wu, and Fan Zhou. Mining spatio-temporal relations via self-paced graph contrastive learning. *Proceedings of the 28th ACM SIGKDD Conference on Knowledge Discovery and Data Mining*, 2022. URL https://api.semanticscholar.org/CorpusID:251518220.
- [37] Yuxuan Liang, Kun Ouyang, Junkai Sun, Yiwei Wang, Junbo Zhang, Yu Zheng, David Rosenblum, and Roger Zimmermann. Fine-grained urban flow prediction. In *Proceedings of the Web Conference 2021*, pages 1833–1845, 2021.
- [38] Wei Liu, Yu Zheng, Sanjay Chawla, Jing Yuan, and Xie Xing. Discovering spatio-temporal causal interactions in traffic data streams. In *Proceedings of the 17th ACM SIGKDD international conference on Knowledge discovery and data mining*, pages 1010–1018, 2011.
- [39] Xu Liu, Yutong Xia, Yuxuan Liang, Junfeng Hu, Yiwei Wang, Lei Bai, Chao Huang, Zhenguang Liu, Bryan Hooi, and Roger Zimmermann. Largest: A benchmark dataset for large-scale traffic forecasting. *Advances in Neural Information Processing Systems*, 36, 2024.
- [40] Xiaoxiao Long, Yuan-Chen Guo, Cheng Lin, Yuan Liu, Zhiyang Dou, Lingjie Liu, Yuexin Ma, Song-Hai Zhang, Marc Habermann, Christian Theobalt, et al. Wonder3d: Single image to 3d using cross-domain diffusion. In *Proceedings of the IEEE/CVF Conference on Computer Vision and Pattern Recognition*, pages 9970–9980, 2024.
- [41] Cheng Lu, Yuhao Zhou, Fan Bao, Jianfei Chen, Chongxuan Li, and Jun Zhu. Dpm-solver++: Fast solver for guided sampling of diffusion probabilistic models. *arXiv* preprint *arXiv*:2211.01095, 2022.
- [42] Andreas Lugmayr, Martin Danelljan, Andres Romero, Fisher Yu, Radu Timofte, and Luc Van Gool. Repaint: Inpainting using denoising diffusion probabilistic models. In *Proceedings of the IEEE/CVF conference on computer vision and pattern recognition*, pages 11461–11471, 2022.
- [43] Dongsheng Luo, Wei Cheng, Dongkuan Xu, Wenchao Yu, Bo Zong, Haifeng Chen, and Xiang Zhang. Parameterized explainer for graph neural network. *Advances in neural information processing systems*, 33:19620–19631, 2020.

- [44] Jiayuan Luo, Wentao Zhang, Yuchen Fang, Xiaowei Gao, Dingyi Zhuang, Hao Chen, and Xinke Jiang. Timeseries suppliers allocation risk optimization via deep black litterman model. ArXiv, abs/2401.17350, 2024. URL https://api.semanticscholar.org/CorpusID: 271854629.
- [45] Michael Mathieu, Camille Couprie, and Yann LeCun. Deep multi-scale video prediction beyond mean square error. *arXiv preprint arXiv:1511.05440*, 2015.
- [46] Alex Nichol, Prafulla Dhariwal, Aditya Ramesh, Pranav Shyam, Pamela Mishkin, Bob Mc-Grew, Ilya Sutskever, and Mark Chen. Glide: Towards photorealistic image generation and editing with text-guided diffusion models. *arXiv preprint arXiv:2112.10741*, 2021.
- [47] Peer Nowack, Jakob Runge, Veronika Eyring, and Joanna D Haigh. Causal networks for climate model evaluation and constrained projections. *Nature communications*, 11(1):1415, 2020.
- [48] Junhyuk Oh, Xiaoxiao Guo, Honglak Lee, Richard L Lewis, and Satinder Singh. Action-conditional video prediction using deep networks in atari games. *Advances in neural information processing systems*, 28, 2015.
- [49] Deepak Pathak, Philipp Krahenbuhl, Jeff Donahue, Trevor Darrell, and Alexei A Efros. Context encoders: Feature learning by inpainting. In *Proceedings of the IEEE conference on computer vision and pattern recognition*, pages 2536–2544, 2016.
- [50] Jaideep Pathak, Shashank Subramanian, Peter Harrington, Sanjeev Raja, Ashesh Chattopadhyay, Morteza Mardani, Thorsten Kurth, David Hall, Zongyi Li, Kamyar Azizzadenesheli, et al. Fourcastnet: A global data-driven high-resolution weather model using adaptive fourier neural operators. *arXiv preprint arXiv:2202.11214*, 2022.
- [51] Judea Pearl. Causality. Cambridge university press, 2009.
- [52] Judea Pearl and Dana Mackenzie. *The book of why: the new science of cause and effect.* Basic books, 2018.
- [53] Roger W Pryor. *Multiphysics modeling using COMSOL®: a first principles approach.* Jones & Bartlett Publishers, 2009.
- [54] Maziar Raissi, Paris Perdikaris, and George E Karniadakis. Physics-informed neural networks: A deep learning framework for solving forward and inverse problems involving nonlinear partial differential equations. *Journal of Computational physics*, 378:686–707, 2019.
- [55] Elad Richardson, Yuval Alaluf, Or Patashnik, Yotam Nitzan, Yaniv Azar, Stav Shapiro, and Daniel Cohen-Or. Encoding in style: a stylegan encoder for image-to-image translation. In *Proceedings of the IEEE/CVF conference on computer vision and pattern recognition*, pages 2287–2296, 2021.
- [56] Shiori Sagawa, Pang Wei Koh, Tatsunori B Hashimoto, and Percy Liang. Distributionally robust neural networks for group shifts: On the importance of regularization for worst-case generalization. *arXiv* preprint arXiv:1911.08731, 2019.
- [57] Chitwan Saharia, William Chan, Huiwen Chang, Chris Lee, Jonathan Ho, Tim Salimans, David Fleet, and Mohammad Norouzi. Palette: Image-to-image diffusion models. In *ACM SIGGRAPH 2022 conference proceedings*, pages 1–10, 2022.
- [58] Christian Schuldt, Ivan Laptev, and Barbara Caputo. Recognizing human actions: a local svm approach. In *Proceedings of the 17th International Conference on Pattern Recognition*, 2004. *ICPR 2004*., volume 3, pages 32–36. IEEE, 2004.
- [59] Martin G Schultz, Clara Betancourt, Bing Gong, Felix Kleinert, Michael Langguth, Lukas Hubert Leufen, Amirpasha Mozaffari, and Scarlet Stadtler. Can deep learning beat numerical weather prediction? *Philosophical Transactions of the Royal Society A*, 379(2194):20200097, 2021.

- [60] Ramprasaath R Selvaraju, Abhishek Das, Ramakrishna Vedantam, Michael Cogswell, Devi Parikh, and Dhruv Batra. Grad-cam: Why did you say that? arXiv preprint arXiv:1611.07450, 2016
- [61] Ramprasaath R Selvaraju, Michael Cogswell, Abhishek Das, Ramakrishna Vedantam, Devi Parikh, and Dhruv Batra. Grad-cam: Visual explanations from deep networks via gradient-based localization. In *Proceedings of the IEEE international conference on computer vision*, pages 618–626, 2017.
- [62] Fei Shen, Hu Ye, Jun Zhang, Cong Wang, Xiao Han, and Yang Wei. Advancing pose-guided image synthesis with progressive conditional diffusion models. In *The Twelfth International Conference on Learning Representations*, 2023.
- [63] Fei Shen, Xin Jiang, Xin He, Hu Ye, Cong Wang, Xiaoyu Du, Zechao Li, and Jinghui Tang. Imagdressing-v1: Customizable virtual dressing. arXiv preprint arXiv:2407.12705, 2024.
- [64] Fei Shen, Hu Ye, Sibo Liu, Jun Zhang, Cong Wang, Xiao Han, and Wei Yang. Boosting consistency in story visualization with rich-contextual conditional diffusion models. arXiv preprint arXiv:2407.02482, 2024.
- [65] Xingjian Shi, Zhourong Chen, Hao Wang, Dit-Yan Yeung, Wai-Kin Wong, and Wang-chun Woo. Convolutional 1stm network: A machine learning approach for precipitation nowcasting. Advances in neural information processing systems, 28, 2015.
- [66] Shohei Shimizu, Patrik O Hoyer, Aapo Hyvärinen, Antti Kerminen, and Michael Jordan. A linear non-gaussian acyclic model for causal discovery. *Journal of Machine Learning Research*, 7(10), 2006.
- [67] Jiaming Song, Chenlin Meng, and Stefano Ermon. Denoising diffusion implicit models. arXiv preprint arXiv:2010.02502, 2020.
- [68] Yang Song, Jascha Sohl-Dickstein, Diederik P Kingma, Abhishek Kumar, Stefano Ermon, and Ben Poole. Score-based generative modeling through stochastic differential equations. *arXiv* preprint arXiv:2011.13456, 2020.
- [69] Nitish Srivastava, Elman Mansimov, and Ruslan Salakhudinov. Unsupervised learning of video representations using lstms. In *International conference on machine learning*, pages 843–852. PMLR, 2015.
- [70] Makoto Takamoto, Francesco Alesiani, and Mathias Niepert. Cape: Channel-attention-based pde parameter embeddings for sciml. 2022.
- [71] Wai Cheong Tam, Eugene Yujun Fu, Jiajia Li, Xinyan Huang, Jian Chen, and Michael Xuelin Huang. A spatial temporal graph neural network model for predicting flashover in arbitrary building floorplans. *Engineering Applications of Artificial Intelligence*, 115:105258, 2022.
- [72] Cheng Tan, Zhangyang Gao, Lirong Wu, Yongjie Xu, Jun Xia, Siyuan Li, and Stan Z Li. Temporal attention unit: Towards efficient spatiotemporal predictive learning. In *Proceedings* of the IEEE/CVF Conference on Computer Vision and Pattern Recognition, pages 18770– 18782, 2023.
- [73] Yiwen Tang, Jiaming Liu, Dong Wang, Zhigang Wang, Shanghang Zhang, Bin Zhao, and Xuelong Li. Any2point: Empowering any-modality large models for efficient 3d understanding. arXiv preprint arXiv:2404.07989, 2024.
- [74] Yiwen Tang, Ray Zhang, Zoey Guo, Xianzheng Ma, Bin Zhao, Zhigang Wang, Dong Wang, and Xuelong Li. Point-peft: Parameter-efficient fine-tuning for 3d pre-trained models. In Proceedings of the AAAI Conference on Artificial Intelligence, volume 38, pages 5171–5179, 2024.
- [75] Xavier-Andoni Tibau, Christian Reimers, Andreas Gerhardus, Joachim Denzler, Veronika Eyring, and Jakob Runge. A spatiotemporal stochastic climate model for benchmarking causal discovery methods for teleconnections. *Environmental Data Science*, 1:e12, 2022.

- [76] Hugo Touvron, Thibaut Lavril, Gautier Izacard, Xavier Martinet, Marie-Anne Lachaux, Timothée Lacroix, Baptiste Rozière, Naman Goyal, Eric Hambro, Faisal Azhar, et al. Llama: Open and efficient foundation language models. *arXiv preprint arXiv:2302.13971*, 2023.
- [77] Sergey Tulyakov, Ming-Yu Liu, Xiaodong Yang, and Jan Kautz. Mocogan: Decomposing motion and content for video generation. In *Proceedings of the IEEE conference on computer vision and pattern recognition*, pages 1526–1535, 2018.
- [78] Ashish Vaswani, Noam Shazeer, Niki Parmar, Jakob Uszkoreit, Llion Jones, Aidan N Gomez, Łukasz Kaiser, and Illia Polosukhin. Attention is all you need. *Advances in neural information processing systems*, 30, 2017.
- [79] Mark Veillette, Siddharth Samsi, and Chris Mattioli. Sevir: A storm event imagery dataset for deep learning applications in radar and satellite meteorology. Advances in Neural Information Processing Systems, 33:22009–22019, 2020.
- [80] Ruben Villegas, Dumitru Erhan, Honglak Lee, et al. Hierarchical long-term video prediction without supervision. In *International Conference on Machine Learning*, pages 6038–6046. PMLR, 2018.
- [81] Hanchen Wang, Tianfan Fu, Yuanqi Du, Wenhao Gao, Kexin Huang, Ziming Liu, Payal Chandak, Shengchao Liu, Peter Van Katwyk, Andreea Deac, et al. Scientific discovery in the age of artificial intelligence. *Nature*, 620(7972):47–60, 2023.
- [82] Kun Wang, Hao Wu, Yifan Duan, Guibin Zhang, Kai Wang, Xiaojiang Peng, Yu Zheng, Yuxuan Liang, and Yang Wang. Nuwadynamics: Discovering and updating in causal spatio-temporal modeling.
- [83] Kun Wang, Guibin Zhang, Xinnan Zhang, Junfeng Fang, Xun Wu, Guohao Li, Shirui Pan, Wei Huang, and Yuxuan Liang. The heterophilic snowflake hypothesis: Training and empowering gnns for heterophilic graphs. In *Proceedings of the 30th ACM SIGKDD Conference on Knowledge Discovery and Data Mining*, pages 3164–3175, 2024.
- [84] Senzhang Wang, Jiannong Cao, and S Yu Philip. Deep learning for spatio-temporal data mining: A survey. *IEEE transactions on knowledge and data engineering*, 34(8):3681–3700, 2020.
- [85] Yaqing Wang, Quanming Yao, James T Kwok, and Lionel M Ni. Generalizing from a few examples: A survey on few-shot learning. *ACM computing surveys (csur)*, 53(3):1–34, 2020.
- [86] Yunbo Wang, Haixu Wu, Jianjin Zhang, Zhifeng Gao, Jianmin Wang, S Yu Philip, and Mingsheng Long. Predrnn: A recurrent neural network for spatiotemporal predictive learning. *IEEE Transactions on Pattern Analysis and Machine Intelligence*, 45(2):2208–2225, 2022.
- [87] Zepu Wang, Peng Sun, Yulin Hu, and Azzedine Boukerche. Sfl: A high-precision traffic flow predictor for supporting intelligent transportation systems. In *GLOBECOM 2022-2022 IEEE Global Communications Conference*, pages 251–256. IEEE, 2022.
- [88] Zepu Wang, Yifei Sun, Zhiyu Lei, Xincheng Zhu, and Peng Sun. Sst: A simplified swin transformer-based model for taxi destination prediction based on existing trajectory. In 2023 IEEE 26th International Conference on Intelligent Transportation Systems (ITSC), pages 1404–1409. IEEE, 2023.
- [89] Qingsong Wen, Tian Zhou, Chaoli Zhang, Weiqi Chen, Ziqing Ma, Junchi Yan, and Liang Sun. Transformers in time series: A survey. *arXiv preprint arXiv:2202.07125*, 2022.
- [90] Hao Wu, Kun Wang, Fan Xu, Yue Li, Xu Wang, Weiyan Wang, Haixin Wang, and Xiao Luo. Spatio-temporal twins with a cache for modeling long-term system dynamics. 2023.
- [91] Hao Wu, Wei Xion, Fan Xu, Xiao Luo, Chong Chen, Xian-Sheng Hua, and Haixin Wang. Pastnet: Introducing physical inductive biases for spatio-temporal video prediction. *arXiv* preprint arXiv:2305.11421, 2023.

- [92] Hao Wu, Yuxuan Liang, Wei Xiong, Zhengyang Zhou, Wei Huang, Shilong Wang, and Kun Wang. Earthfarsser: Versatile spatio-temporal dynamical systems modeling in one model. In *Proceedings of the AAAI Conference on Artificial Intelligence*, volume 38, pages 15906–15914, 2024.
- [93] Hao Wu, Haomin Wen, Guibin Zhang, Yutong Xia, Kai Wang, Yuxuan Liang, Yu Zheng, and Kun Wang. Dynst: Dynamic sparse training for resource-constrained spatio-temporal forecasting. *arXiv preprint arXiv:2403.02914*, 2024.
- [94] Ying-Xin Wu, Xiang Wang, An Zhang, Xia Hu, Fuli Feng, Xiangnan He, and Tat-Seng Chua. Deconfounding to explanation evaluation in graph neural networks. *arXiv preprint arXiv:2201.08802*, 2022.
- [95] Yutong Xia, Yuxuan Liang, Haomin Wen, Xu Liu, Kun Wang, Zhengyang Zhou, and Roger Zimmermann. Deciphering spatio-temporal graph forecasting: A causal lens and treatment. *Advances in Neural Information Processing Systems*, 36, 2024.
- [96] Songhua Yang, Xinke Jiang, Hanjie Zhao, Wenxuan Zeng, Hongde Liu, and Yuxiang Jia. Faima: Feature-aware in-context learning for multi-domain aspect-based sentiment analysis. *ArXiv*, abs/2403.01063, 2024. URL https://api.semanticscholar.org/CorpusID: 268230305.
- [97] Zhitao Ying, Dylan Bourgeois, Jiaxuan You, Marinka Zitnik, and Jure Leskovec. Gnnexplainer: Generating explanations for graph neural networks. *Advances in neural information processing systems*, 32, 2019.
- [98] Guibin Zhang, Kun Wang, Wei Huang, Yanwei Yue, Yang Wang, Roger Zimmermann, Aojun Zhou, Dawei Cheng, Jin Zeng, and Yuxuan Liang. Graph lottery ticket automated. In *The Twelfth International Conference on Learning Representations*, 2024.
- [99] Guibin Zhang, Yanwei Yue, Kun Wang, Junfeng Fang, Yongduo Sui, Kai Wang, Yuxuan Liang, Dawei Cheng, Shirui Pan, and Tianlong Chen. Two heads are better than one: Boosting graph sparse training via semantic and topological awareness. *arXiv preprint arXiv:2402.01242*, 2024.
- [100] Hongyi Zhang, Moustapha Cisse, Yann N Dauphin, and David Lopez-Paz. mixup: Beyond empirical risk minimization. *arXiv preprint arXiv:1710.09412*, 2017.
- [101] Lei Zhao, Qihang Mo, Sihuan Lin, Zhizhong Wang, Zhiwen Zuo, Haibo Chen, Wei Xing, and Dongming Lu. Uctgan: Diverse image inpainting based on unsupervised cross-space translation. In *Proceedings of the IEEE/CVF conference on computer vision and pattern recognition*, pages 5741–5750, 2020.
- [102] Shengyu Zhao, Jonathan Cui, Yilun Sheng, Yue Dong, Xiao Liang, Eric I Chang, and Yan Xu. Large scale image completion via co-modulated generative adversarial networks. arXiv preprint arXiv:2103.10428, 2021.
- [103] Chuanxia Zheng, Tat-Jen Cham, and Jianfei Cai. Pluralistic image completion. In *Proceedings* of the IEEE/CVF Conference on Computer Vision and Pattern Recognition, pages 1438–1447, 2019.
- [104] Xun Zheng, Bryon Aragam, Pradeep K Ravikumar, and Eric P Xing. Dags with no tears: Continuous optimization for structure learning. *Advances in neural information processing systems*, 31, 2018.
- [105] Yiqi Zhong, Luming Liang, Ilya Zharkov, and Ulrich Neumann. Mmvp: Motion-matrix-based video prediction. In *Proceedings of the IEEE/CVF International Conference on Computer Vision*, pages 4273–4283, 2023.
- [106] Zhengyang Zhou, Qihe Huang, Kuo Yang, Kun Wang, Xu Wang, Yudong Zhang, Yuxuan Liang, and Yang Wang. Maintaining the status quo: Capturing invariant relations for ood spatiotemporal learning. In *Proceedings of the 29th ACM SIGKDD Conference on Knowledge Discovery and Data Mining*, pages 3603–3614, 2023.

A CaPaint Inpainting Algorithm

Algorithm 1 Causal Intervention with Diffusion Inpainting

```
1: Input: ST observation data X, masked image X_{mask}
 2: Output: Augmentation ST observation dataset X_A
 3: Initialize X_T \sim \mathcal{N}(0, I) where T is the total number of diffusion steps
 4: /* Iterate backwards through diffusion steps */
 5: for t = T to 1 do
          /* Sample Gaussian noise \epsilon */
 7:
          \epsilon \sim \mathcal{N}(0, I)
          /* Sample causal region */
 8:
 9:
          X_{t-1}^{cau} = \sqrt{\bar{\alpha}_t} X_0 + (1 - \bar{\alpha}_t) \epsilon
10:
          /* Sample Gaussian noise N */
11:
          z \sim \mathcal{N}(0, I)
12:
          /* Causal Intervention on Environmental Patches */
          X_{t-1}^{env} = \frac{1}{\sqrt{\alpha_t}} \left( X_t - \frac{\beta_t}{\sqrt{1 - \bar{\alpha}_t}} \epsilon_{\theta}(X_t, t) + \sigma_t z \right)
/* Combine causal and environmental patches */
13:
14:
          X_{t-1} = m \odot X_{t-1}^{cau} + (1-m) \odot X_{t-1}^{ent}
15:
          X_t \sim \mathcal{N}(\sqrt{1 - \beta_{t-1}} X_{t-1}, \beta_{t-1} I)
16:
17: end for
18: return X_A as the augmentation dataset
```

The algorithm for **Causal Intervention with Diffusion Inpainting** aims to augment ST observation data through a series of diffusion steps that iteratively refine the data by applying causal interventions and combining them with environmental patches. Here is a detailed step-by-step description:

- Input: The original ST observation data X, and a masked image X_{mask} .
- Output: An augmented ST observation dataset X_A .
- The process begins by initializing X_T , which represents the data at the final diffusion step, to be a sample from a normal distribution centered at zero with identity covariance.
- ullet The main loop of the algorithm runs backward from the last diffusion step T to the first. In each step:
 - 1. Gaussian noise ϵ_t is sampled to simulate the diffusion process.
 - 2. A causal region $X_{\rm cau}$ is sampled where the causal effect is calculated as a blend of the original data and the Gaussian noise, emphasizing areas of interest that should retain more original data characteristics.
 - 3. Gaussian noise N_t is sampled again, providing variability to the non-causal or environmental regions.
 - The environmental patches X_{env} are updated using the data from the previous step adjusted by a damping factor and the added noise, simulating environmental changes.
 - 5. The causal and environmental patches are then combined, where the mask M determines the specific locations for the causal and environmental updates in the data, specifying which parts are from the causal region and which are from the environmental region.
 - 6. The data for the next step, X_{t-1} , is computed by normalizing the combined updates, preparing it for the next iteration or output if it is the first step.
- Finally, the algorithm outputs the augmented data set X_A , which is the result of the iterative causal intervention and environmental blending over the diffusion process.

B Details of experiments

SSIM stands for Structural Similarity Index Measure, which is a method for measuring the similarity between two images. It compares the structural information of the images, including luminance,

contrast, and texture, to determine how similar they are. SSIM is commonly used in image and video processing applications, such as image compression and quality assessment.

PSNR stands for Peak Signal-to-Noise Ratio. It is a measure of video or image quality that compares the original signal to the compressed or transmitted signal. The higher the PSNR value, the better the quality of the compressed or transmitted signal. PSNR is commonly used in video and image compression applications to evaluate the effectiveness of compression algorithms.

MSE (Mean Squared Error) loss is a commonly used loss function in machine learning and deep learning models. This loss function calculates the average of the squared differences between the predicted and actual values.

Datasets. Here we summarize the details (Tab. 1) of the datasets used in this paper:

- TaxiBJ+: This dataset contains trajectory data obtained from the GPS of taxis in Beijing, divided into two separate channels: inflow and outflow. Additionally, the dataset has been extended from 32×32 to 128×128 by collecting recent trajectory data from Beijing.
- KTH: This dataset includes 25 individuals performing six different actions: walking, jogging, running, boxing, waving, and clapping. The complexity of human movements arises from the unique variations each individual displays while executing these actions. By examining previous frames, the model can understand the subtleties of human dynamics and predict future extended postural changes.
- SEVIR: This dataset consists of weather images that have been sampled and aligned using radar and satellite data. It is designed as a foundational resource to support algorithm development in meteorological research.
- DRS: This dataset describes the diffusion process of nonlinear wave, which satisfies the diffusion equation.
- FireSys: The FireSys dataset comprises data associated with fire observations, capturing both temporal and spatial trends of fire evolution, which faithfully represent the progression status in a natural setting.

C Broader Impact

The development and application of the CaPaint framework in spatio-temporal (ST) dynamics bring several positive broader impacts. Understanding these impacts is crucial for responsible AI research and deployment.

- **1. Data Imputation in Sparse Scenarios:** CaPaint excels in sparse data scenarios, effectively filling in missing data. This reduces the need for extensive sensor deployments, significantly lowering the cost associated with sensor installation. By optimizing data coverage and utilization, CaPaint not only enhances resource efficiency but also achieves substantial cost savings.
- 2. Enhanced Predictive Accuracy and Interpretability: CaPaint can identify and intervene in non-causal regions, improving the predictive accuracy and interpretability in various ST domains such as meteorology, human mobility, and disaster management. This improvement leads to better decision-making processes and resource allocation, ultimately benefiting society by providing more reliable and understandable predictive models.
- **3. Cost-Effective Solutions:** By reducing the complexity of optimal ST causal discovery models, CaPaint offers a cost-effective solution for handling high-dimensional ST data. This makes advanced predictive technologies more accessible across a broader range of applications, particularly in fields with limited computational resources.
- **4. Promotion of Causal Reasoning in AI:** The integration of causal reasoning into ST models encourages the development of AI systems that better mimic human understanding of cause-and-effect relationships. This can lead to more robust AI models capable of generalizing across different scenarios, fostering trust and reliability in AI applications.
- **5. Innovation in Data Augmentation Techniques:** CaPaint introduces novel data augmentation methods using diffusion inpainting, which can inspire further research and innovation in data augmentation and ST prediction. This can lead to the emergence of new techniques, enhancing the robustness and performance of AI models in various domains.

The CaPaint framework represents a significant advancement in the field of ST dynamics, particularly in its ability to address sparse data scenarios, which reduces the need for extensive sensor deployments and lowers associated costs. Additionally, CaPaint enhances predictive accuracy, interpretability, and efficiency, promotes causal reasoning in AI, and introduces innovative data augmentation techniques. Responsible AI research and deployment should leverage these strengths to maximize benefits while minimizing risks.

D Metrics

In our research, we investigate the performance of our models using Mean Squared Error (MSE), Mean Absolute Error (MAE), and Structural Similarity Index Measure (SSIM). The formulas for evaluating these indicators, converted into decibels (dB) where applicable, are as follows:

Mean Squared Error (MSE)

Mean Squared Error (MSE) measures the average of the squares of the errors, that is, the average squared difference between the estimated values and the actual value. The MSE is given by:

$$MSE = \frac{1}{N} \sum_{i=1}^{N} (Y_i - \hat{Y}_i)^2$$
 (D.1)

where Y_i is the actual value, \hat{Y}_i is the predicted value, and N is the number of observations.

Mean Absolute Error (MAE)

Mean Absolute Error (MAE) measures the average magnitude of the errors in a set of predictions, without considering their direction. It is the average over the test sample of the absolute differences between prediction and actual observation where all individual differences have equal weight. The MAE is given by:

$$MAE = \frac{1}{N} \sum_{i=1}^{N} \left| Y_i - \hat{Y}_i \right|$$
 (D.2)

where Y_i is the actual value, \hat{Y}_i is the predicted value, and N is the number of observations.

Structural Similarity Index Measure (SSIM)

Structural Similarity Index Measure (SSIM) is used for measuring the similarity between two images. The SSIM index is a decimal value between -1 and 1, where 1 is only reachable in the case of two identical sets of data. The SSIM formula can be quite complex due to its consideration of luminance, contrast, and structure comparison functions between the two images:

$$SSIM(x,y) = \frac{(2\mu_x \mu_y + C_1)(2\sigma_{xy} + C_2)}{(\mu_x^2 + \mu_y^2 + C_1)(\sigma_x^2 + \sigma_y^2 + C_2)}$$
(D.3)

where μ_x , μ_y are the average of x and y respectively, σ_x^2 , σ_y^2 are the variance of x and y respectively, σ_{xy} is the covariance of x and y, and C_1, C_2 are variables to stabilize the division with weak denominator.

E Limitations

While the implementation of the CaPaint method has demonstrated significant improvements in prediction accuracy and detail preservation in spatio-temporal forecasting tasks, its enhancements are most pronounced in scenarios characterized by data scarcity or uneven data distribution. In contexts where datasets are abundant and exhibit a broad and uniform distribution, the incremental gains offered by CaPaint may not be as substantial. Nevertheless, the method remains effective, providing consistent, albeit smaller, improvements across diverse data environments.

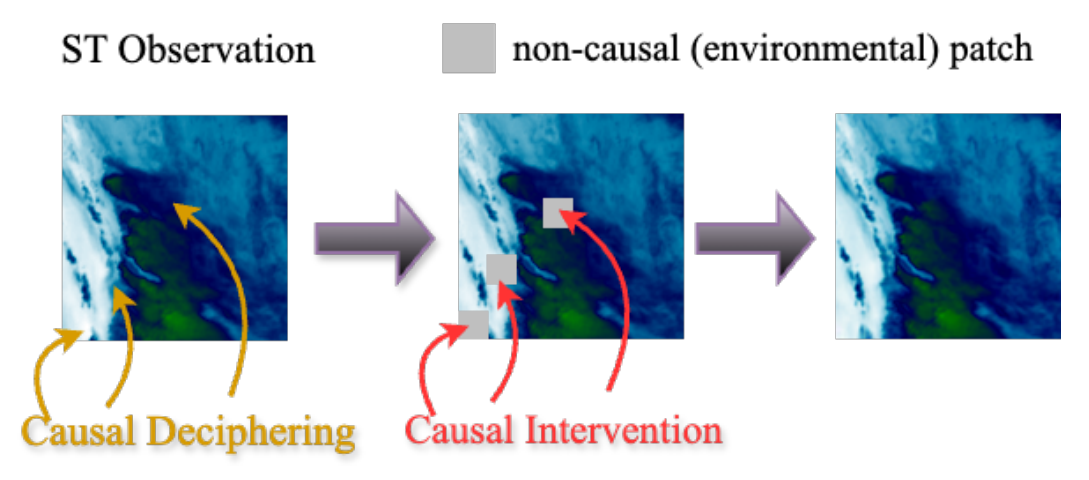


Figure F.1: Inpainting Example of our proposed CaPaint.

F An example of ST Inpainting on SEVIR

The figure illustrates the process of maintaining causal regions intact while performing inpainting on non-causal (environmental) regions. The approach involves identifying and deciphering the causal regions (left), intervening by applying diffusion inpainting on the environmental patches (middle), and subsequently generating altered ST data copies (right). This method ensures that the intrinsic causal relationships within the data are preserved, while variations are introduced in the environmental context to augment the dataset effectively.

G Uneven Distribution of Sensors Leading to Data Scarcity in Global Oceanic Observation

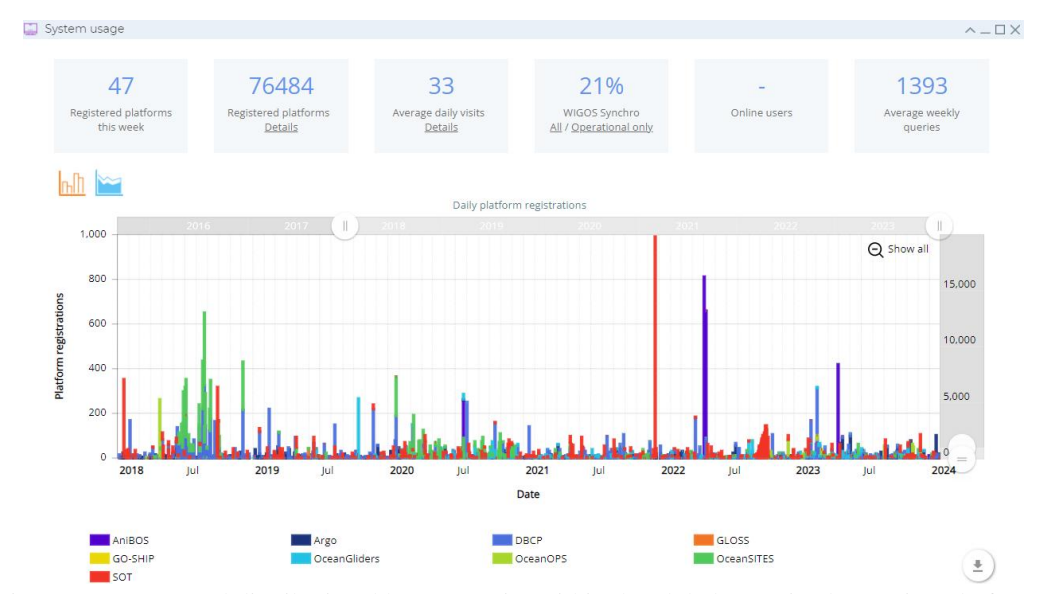


Figure G.1: Temporal distributional heterogeneity within the global oceanic observation platforms, which reveals that there are pronounced disparities in the deployment numbers of various types of sensors during different time intervals.

H Experimental Parameters

In this experiment, we employ different deep learning models and optimize them for training. All experiments are conducted on hardware equipped with 24 NVIDIA GeForce RTX 4090 GPUs. The optimizer used is Adam, and different learning rates (LR) and batch sizes are set for each model. The specific parameter settings are shown in the table below:

Model	Learning Rate (LR)	Batch Size
CLSTM	0.001	8
MAU	0.001	8
MMVP	0.004	4
PredRNNv2	0.001	8
SimVP	0.004	4
ViT	0.004	4
Earthfarsser	0.001	8

Table H.1: Learning rates and batch sizes for different backbones

These parameter settings are chosen based on the characteristics of each model and preliminary experimental results on the validation set, aiming to optimize the training efficiency and performance of the models. The Adam optimizer is used with a OneCycle learning rate scheduler, where the maximum learning rate is set according to the specified learning rate for each model, and the number of steps per epoch and the total number of epochs are set based on the training data and experimental setup. During the experiments, we ensure that all models are trained under the same hardware conditions to guarantee the comparability and reproducibility of the results.

I Visualizations on KTH



Figure I.1: Visualizations on KTH dataset showing the last 5 frames

The first row shows the ground truth for a walking individual. The second row, processed by Earthfarser, exhibits noticeable blurring and loss of detail. The third row, enhanced with +CaPaint, demonstrates a marked improvement in capturing fine details such as the shadow of the person and the accuracy of the foot motion, as highlighted in the red boxes.

J Visualizations on Diffusion Reaction System

The introduction of CaPaint has led to reductions in Mean Squared Error MSE and MAE, while the SSIM has shown improvements. These changes indicate that the CaPaint method effectively enhances model prediction accuracy and image quality. However, due to the high quality of the model predictions, the improvements might not be readily observable to the naked eye. Despite this, the

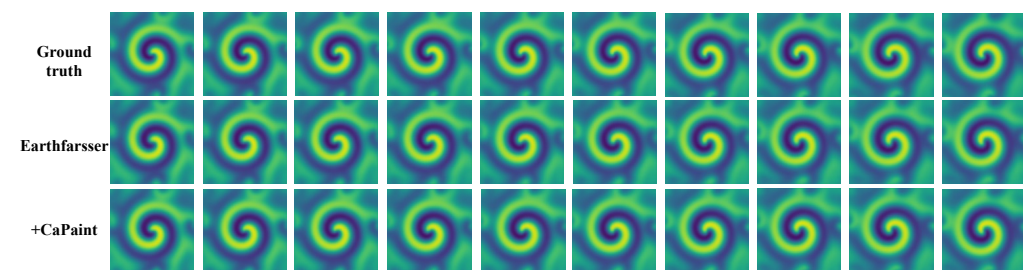


Figure J.1: Visualizations on DRS dataset showing 10 frames

positive effects of CaPaint are clearly evident through quantitative metrics, demonstrating its potential and practicality in enhancing the accuracy of complex dynamic systems predictions.

NeurIPS Paper Checklist

1. Claims

Question: Do the main claims made in the abstract and introduction accurately reflect the paper's contributions and scope?

Answer: [Yes]

Justification: In this paper, we introduce the spatio-temporal causal concept in the data mining realm, aimed at enhancing the reliability and accuracy of financial spatio-temporal prediction.

Guidelines:

- The answer NA means that the abstract and introduction do not include the claims made in the paper.
- The abstract and/or introduction should clearly state the claims made, including the
 contributions made in the paper and important assumptions and limitations. A No or
 NA answer to this question will not be perceived well by the reviewers.
- The claims made should match theoretical and experimental results, and reflect how much the results can be expected to generalize to other settings.
- It is fine to include aspirational goals as motivation as long as it is clear that these goals are not attained by the paper.

2. Limitations

Question: Does the paper discuss the limitations of the work performed by the authors?

Answer: [Yes]

Justification: In this work, we systematically discuss the limitations of our research and outline directions for future work.

Guidelines:

- The answer NA means that the paper has no limitation while the answer No means that the paper has limitations, but those are not discussed in the paper.
- The authors are encouraged to create a separate "Limitations" section in their paper.
- The paper should point out any strong assumptions and how robust the results are to violations of these assumptions (e.g., independence assumptions, noiseless settings, model well-specification, asymptotic approximations only holding locally). The authors should reflect on how these assumptions might be violated in practice and what the implications would be.
- The authors should reflect on the scope of the claims made, e.g., if the approach was only tested on a few datasets or with a few runs. In general, empirical results often depend on implicit assumptions, which should be articulated.
- The authors should reflect on the factors that influence the performance of the approach. For example, a facial recognition algorithm may perform poorly when image resolution is low or images are taken in low lighting. Or a speech-to-text system might not be used reliably to provide closed captions for online lectures because it fails to handle technical jargon.
- The authors should discuss the computational efficiency of the proposed algorithms and how they scale with dataset size.
- If applicable, the authors should discuss possible limitations of their approach to address problems of privacy and fairness.
- While the authors might fear that complete honesty about limitations might be used by reviewers as grounds for rejection, a worse outcome might be that reviewers discover limitations that aren't acknowledged in the paper. The authors should use their best judgment and recognize that individual actions in favor of transparency play an important role in developing norms that preserve the integrity of the community. Reviewers will be specifically instructed to not penalize honesty concerning limitations.

3. Theory Assumptions and Proofs

Question: For each theoretical result, does the paper provide the full set of assumptions and a complete (and correct) proof?

Answer: [NA]

Justification: This paper does not include experimental results related to theoretical aspects. Guidelines:

- The answer NA means that the paper does not include theoretical results.
- All the theorems, formulas, and proofs in the paper should be numbered and crossreferenced.
- All assumptions should be clearly stated or referenced in the statement of any theorems.
- The proofs can either appear in the main paper or the supplemental material, but if they appear in the supplemental material, the authors are encouraged to provide a short proof sketch to provide intuition.
- Inversely, any informal proof provided in the core of the paper should be complemented by formal proofs provided in appendix or supplemental material.
- Theorems and Lemmas that the proof relies upon should be properly referenced.

4. Experimental Result Reproducibility

Question: Does the paper fully disclose all the information needed to reproduce the main experimental results of the paper to the extent that it affects the main claims and/or conclusions of the paper (regardless of whether the code and data are provided or not)?

Answer: [Yes]

Justification: We provide the code necessary for replicating the studies described in this paper via an anonymous link, and we detail the experimental setup for the replication in the article itself.

Guidelines:

- The answer NA means that the paper does not include experiments.
- If the paper includes experiments, a No answer to this question will not be perceived well by the reviewers: Making the paper reproducible is important, regardless of whether the code and data are provided or not.
- If the contribution is a dataset and/or model, the authors should describe the steps taken to make their results reproducible or verifiable.
- Depending on the contribution, reproducibility can be accomplished in various ways. For example, if the contribution is a novel architecture, describing the architecture fully might suffice, or if the contribution is a specific model and empirical evaluation, it may be necessary to either make it possible for others to replicate the model with the same dataset, or provide access to the model. In general, releasing code and data is often one good way to accomplish this, but reproducibility can also be provided via detailed instructions for how to replicate the results, access to a hosted model (e.g., in the case of a large language model), releasing of a model checkpoint, or other means that are appropriate to the research performed.
- While NeurIPS does not require releasing code, the conference does require all submissions to provide some reasonable avenue for reproducibility, which may depend on the nature of the contribution. For example
 - (a) If the contribution is primarily a new algorithm, the paper should make it clear how to reproduce that algorithm.
- (b) If the contribution is primarily a new model architecture, the paper should describe the architecture clearly and fully.
- (c) If the contribution is a new model (e.g., a large language model), then there should either be a way to access this model for reproducing the results or a way to reproduce the model (e.g., with an open-source dataset or instructions for how to construct the dataset).
- (d) We recognize that reproducibility may be tricky in some cases, in which case authors are welcome to describe the particular way they provide for reproducibility. In the case of closed-source models, it may be that access to the model is limited in some way (e.g., to registered users), but it should be possible for other researchers to have some path to reproducing or verifying the results.

5. Open access to data and code

Question: Does the paper provide open access to the data and code, with sufficient instructions to faithfully reproduce the main experimental results, as described in supplemental material?

Answer: [Yes]

Justification: For the datasets disclosed in the article, we have provided information regarding their sources and origins.

Guidelines:

- The answer NA means that paper does not include experiments requiring code.
- Please see the NeurIPS code and data submission guidelines (https://nips.cc/public/guides/CodeSubmissionPolicy) for more details.
- While we encourage the release of code and data, we understand that this might not be possible, so "No" is an acceptable answer. Papers cannot be rejected simply for not including code, unless this is central to the contribution (e.g., for a new open-source benchmark).
- The instructions should contain the exact command and environment needed to run to reproduce the results. See the NeurIPS code and data submission guidelines (https://nips.cc/public/guides/CodeSubmissionPolicy) for more details.
- The authors should provide instructions on data access and preparation, including how
 to access the raw data, preprocessed data, intermediate data, and generated data, etc.
- The authors should provide scripts to reproduce all experimental results for the new proposed method and baselines. If only a subset of experiments are reproducible, they should state which ones are omitted from the script and why.
- At submission time, to preserve anonymity, the authors should release anonymized versions (if applicable).
- Providing as much information as possible in supplemental material (appended to the paper) is recommended, but including URLs to data and code is permitted.

6. Experimental Setting/Details

Question: Does the paper specify all the training and test details (e.g., data splits, hyperparameters, how they were chosen, type of optimizer, etc.) necessary to understand the results?

Answer: [Yes]

Justification: we have specified all the training and test details (e.g., data splits, hyper-parameters, how they were chosen, type of optimizer, etc.) necessary to understand the results.

Guidelines:

- The answer NA means that the paper does not include experiments.
- The experimental setting should be presented in the core of the paper to a level of detail that is necessary to appreciate the results and make sense of them.
- The full details can be provided either with the code, in appendix, or as supplemental material.

7. Experiment Statistical Significance

Question: Does the paper report error bars suitably and correctly defined or other appropriate information about the statistical significance of the experiments?

Answer: [Yes]

Justification: In this paper, we have reported error bars suitably and correctly defined or other appropriate information about the statistical significance of the experiments.

Guidelines:

- The answer NA means that the paper does not include experiments.
- The authors should answer "Yes" if the results are accompanied by error bars, confidence intervals, or statistical significance tests, at least for the experiments that support the main claims of the paper.

- The factors of variability that the error bars are capturing should be clearly stated (for example, train/test split, initialization, random drawing of some parameter, or overall run with given experimental conditions).
- The method for calculating the error bars should be explained (closed form formula, call to a library function, bootstrap, etc.)
- The assumptions made should be given (e.g., Normally distributed errors).
- It should be clear whether the error bar is the standard deviation or the standard error
 of the mean.
- It is OK to report 1-sigma error bars, but one should state it. The authors should preferably report a 2-sigma error bar than state that they have a 96% CI, if the hypothesis of Normality of errors is not verified.
- For asymmetric distributions, the authors should be careful not to show in tables or figures symmetric error bars that would yield results that are out of range (e.g. negative error rates).
- If error bars are reported in tables or plots, The authors should explain in the text how they were calculated and reference the corresponding figures or tables in the text.

8. Experiments Compute Resources

Question: For each experiment, does the paper provide sufficient information on the computer resources (type of compute workers, memory, time of execution) needed to reproduce the experiments?

Answer: [Yes]

Justification: In this paper, we provide detailed information about the experimental resources, including GPU configurations used in our studies.

Guidelines:

- The answer NA means that the paper does not include experiments.
- The paper should indicate the type of compute workers CPU or GPU, internal cluster, or cloud provider, including relevant memory and storage.
- The paper should provide the amount of compute required for each of the individual experimental runs as well as estimate the total compute.
- The paper should disclose whether the full research project required more compute than the experiments reported in the paper (e.g., preliminary or failed experiments that didn't make it into the paper).

9. Code Of Ethics

Question: Does the research conducted in the paper conform, in every respect, with the NeurIPS Code of Ethics https://neurips.cc/public/EthicsGuidelines?

Answer: [Yes]

Justification: The study presented in this paper conforms to the NeurIPS Code of Ethics.

Guidelines:

- The answer NA means that the authors have not reviewed the NeurIPS Code of Ethics.
- If the authors answer No, they should explain the special circumstances that require a deviation from the Code of Ethics.
- The authors should make sure to preserve anonymity (e.g., if there is a special consideration due to laws or regulations in their jurisdiction).

10. Broader Impacts

Question: Does the paper discuss both potential positive societal impacts and negative societal impacts of the work performed?

Answer: [Yes]

Justification: We have provided the societal impacts of the work.

Guidelines:

• The answer NA means that there is no societal impact of the work performed.

- If the authors answer NA or No, they should explain why their work has no societal impact or why the paper does not address societal impact.
- Examples of negative societal impacts include potential malicious or unintended uses (e.g., disinformation, generating fake profiles, surveillance), fairness considerations (e.g., deployment of technologies that could make decisions that unfairly impact specific groups), privacy considerations, and security considerations.
- The conference expects that many papers will be foundational research and not tied to particular applications, let alone deployments. However, if there is a direct path to any negative applications, the authors should point it out. For example, it is legitimate to point out that an improvement in the quality of generative models could be used to generate deepfakes for disinformation. On the other hand, it is not needed to point out that a generic algorithm for optimizing neural networks could enable people to train models that generate Deepfakes faster.
- The authors should consider possible harms that could arise when the technology is being used as intended and functioning correctly, harms that could arise when the technology is being used as intended but gives incorrect results, and harms following from (intentional or unintentional) misuse of the technology.
- If there are negative societal impacts, the authors could also discuss possible mitigation strategies (e.g., gated release of models, providing defenses in addition to attacks, mechanisms for monitoring misuse, mechanisms to monitor how a system learns from feedback over time, improving the efficiency and accessibility of ML).

11. Safeguards

Question: Does the paper describe safeguards that have been put in place for responsible release of data or models that have a high risk for misuse (e.g., pretrained language models, image generators, or scraped datasets)?

Answer: [NA]

Justification: This paper does not address issues related to this aspect.

Guidelines:

- The answer NA means that the paper poses no such risks.
- Released models that have a high risk for misuse or dual-use should be released with
 necessary safeguards to allow for controlled use of the model, for example by requiring
 that users adhere to usage guidelines or restrictions to access the model or implementing
 safety filters.
- Datasets that have been scraped from the Internet could pose safety risks. The authors should describe how they avoided releasing unsafe images.
- We recognize that providing effective safeguards is challenging, and many papers do
 not require this, but we encourage authors to take this into account and make a best
 faith effort.

12. Licenses for existing assets

Question: Are the creators or original owners of assets (e.g., code, data, models), used in the paper, properly credited and are the license and terms of use explicitly mentioned and properly respected?

Answer: [Yes]

Justification: All creators and original owners of the assets used in our paper, such as code, data, and models, have been properly credited. We have explicitly mentioned the licenses and terms of use for each asset and have ensured full compliance with these terms throughout our research.

Guidelines:

- The answer NA means that the paper does not use existing assets.
- The authors should cite the original paper that produced the code package or dataset.
- The authors should state which version of the asset is used and, if possible, include a URL.
- The name of the license (e.g., CC-BY 4.0) should be included for each asset.

- For scraped data from a particular source (e.g., website), the copyright and terms of service of that source should be provided.
- If assets are released, the license, copyright information, and terms of use in the
 package should be provided. For popular datasets, paperswithcode.com/datasets
 has curated licenses for some datasets. Their licensing guide can help determine the
 license of a dataset.
- For existing datasets that are re-packaged, both the original license and the license of the derived asset (if it has changed) should be provided.
- If this information is not available online, the authors are encouraged to reach out to the asset's creators.

13. New Assets

Question: Are new assets introduced in the paper well documented and is the documentation provided alongside the assets?

Answer: [NA]

Justification: The research presented in this paper is not concerned with new assets.

Guidelines:

- The answer NA means that the paper does not release new assets.
- Researchers should communicate the details of the dataset/code/model as part of their submissions via structured templates. This includes details about training, license, limitations, etc.
- The paper should discuss whether and how consent was obtained from people whose asset is used.
- At submission time, remember to anonymize your assets (if applicable). You can either create an anonymized URL or include an anonymized zip file.

14. Crowdsourcing and Research with Human Subjects

Question: For crowdsourcing experiments and research with human subjects, does the paper include the full text of instructions given to participants and screenshots, if applicable, as well as details about compensation (if any)?

Answer: [NA]

Justification: This paper does not involve experiments or research related to human subjects.

Guidelines:

- The answer NA means that the paper does not involve crowdsourcing nor research with human subjects.
- Including this information in the supplemental material is fine, but if the main contribution of the paper involves human subjects, then as much detail as possible should be included in the main paper.
- According to the NeurIPS Code of Ethics, workers involved in data collection, curation, or other labor should be paid at least the minimum wage in the country of the data collector.

15. Institutional Review Board (IRB) Approvals or Equivalent for Research with Human Subjects

Question: Does the paper describe potential risks incurred by study participants, whether such risks were disclosed to the subjects, and whether Institutional Review Board (IRB) approvals (or an equivalent approval/review based on the requirements of your country or institution) were obtained?

Answer: [NA]

Justification: This paper does not address potential risks incurred by study participants.

Guidelines:

 The answer NA means that the paper does not involve crowdsourcing nor research with human subjects.

- Depending on the country in which research is conducted, IRB approval (or equivalent) may be required for any human subjects research. If you obtained IRB approval, you should clearly state this in the paper.
- We recognize that the procedures for this may vary significantly between institutions and locations, and we expect authors to adhere to the NeurIPS Code of Ethics and the guidelines for their institution.
- For initial submissions, do not include any information that would break anonymity (if applicable), such as the institution conducting the review.